THE ROLE OF TGF-BETA SIGNALING IN AN IN VIVO MODEL OF NASH
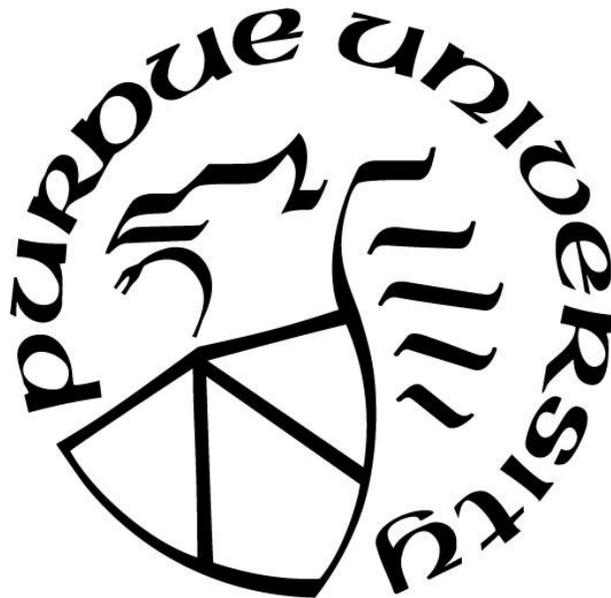
by

Alexander Culver

A Thesis

Submitted to the Faculty of Purdue University

In Partial Fulfillment of the Requirements for the degree of

Master of Science

Department of Biological Sciences

Indianapolis, Indiana

December 2016

THE PURDUE UNIVERSITY GRADUATE SCHOOL
STATEMENT OF THESIS APPROVAL

Dr. Guoli Dai, Chair

      Department of Biology

Dr. James Marrs

      Department of Biology

Dr. Benjamin Yaden

      Department of Biology

Approved by:

      Dr. James Marrs

         Head of the Departmental Graduate Program

Dedicated to Amanda

ACKNOWLEDGEMENTS

TABLE OF CONTENTS

LIST OF FIGURES

LIST OF ABBREVIATIONS

ActRIIA/B-Fc	Ectodomain of ActRIIA or B and Fc-region of immunoglobulin
BMP	Bone morphogenic factor
CCl_4	Carbon tetrachloride
CTGF	Connective tissue growth factor
ECM	Extracellular matrix
FGF21	Fibroblast growth factor 21
FST	Follistatin
Gdf8	Growth differentiation factor 8
Gdf15	Growth differentiation factor 15
HCC	Hepatocellular carcinoma
HSC	Hepatic stellate cell
NASH	Nonalcoholic steatohepatitis
NAFLD	Nonalcoholic fatty liver disease
TGFβ	Tissue growth factor beta

ABSTRACT

Author: Alexander Culver, MS
Institution: Purdue University
Degree Received: December 2016
Title: Tgf-beta Signaling in an *In Vivo* Model of NASH
Major Professor: Guoli Dai

A burgeoning area of focus within liver disease research is centered on the concomitant muscle atrophy present in end stage liver disease patients which shows a correlation to severity of hepatic fibrosis and transplant survival outcomes. Of particular interest, nonalcoholic steatohepatitis (NASH) is a form of liver disease that is characterized as the hepatic manifestation of metabolic syndrome. If left untreated, the disease can progress to the state of cirrhosis and hepatocellular carcinoma requiring transplant. Concordant with increasing global prevalence of obesity, NASH is projected to become the leading cause for liver transplants by 2020. Due to a lack of therapeutic options, these patients represent a large unmet medical need in the western world. A major hurdle to therapeutic research is the lack of a quick, reproducible, and cost effective *in vivo* model that recapitulates the plethora of pathologies and their molecular underpinnings manifested by this disorder. Our studies attempted to validate and expand upon a two-hit model of NASH, which incorporated both the integral comorbidities associated with metabolic challenges of obesity along with liver injury. The two-hit model manifests not only the hepatic morphohistological characteristics of the disease, but also incorporates the obligatory muscle atrophy. To further elaborate on the potential direct link between liver and skeletal muscle and remove any confounding issues associated with the model, *in vitro* administration of hepatotoxins representing various pathologies associated with liver

xi

disease, were used to recapitulate the liver-muscle endocrine signaling that exists *in vivo*. Our data shows that a variety of hepatoxins can elicit hepatocellular damage which releases factors that inhibits myotube size *in vitro*. The two hit model also preserves many of conserved molecular underpinnings observed in clinical hepatic fibrosis. Of particular interest, the TGFβ superfamily has been demonstrated to play an important regulatory role in the progression of fibrosis in NASH patients. TGFβ, Activin A, and Follistatin are members of the highly conserved family that are increased in NASH patients. Furthermore, these proteins have a well-studied role in muscle health, regeneration, and mass that has been hypothesized to be conserved between liver and muscle tissues. Surprisingly, novel expression of the myokine and negative regulator of muscle mass Gdf8 (myostatin) was increased in our *in vivo* model as well. Our studies focused on the molecular interactions of these TGFβ superfamily members and their role on liver disease progression. Through specific inhibition of these proteins (Activin A and Gdf8), we demonstrated that they appear to play key individual roles in the progression of the concomitant muscle atrophy observed in NASH patients. Interestingly, superior efficacy was gained with the treatment of a pan inhibitor of these proteins (Activin A, B, Gdf8 etc.) via a soluble decoy receptor (ActRIIB-Fc), suggesting an additional unaccounted for ligand. Activin B, was found to be increased in two separate *in vivo* models of liver fibrosis (two-hit model and BDL), has been implicated in regulating muscle mass. Our data suggest a pivotal role for several members of the TGFβ superfamily in NASH associated muscle atrophy. Therapies designed to treat liver fibrosis and the resultant decrements in muscle mass and force must account for these

agents which will require pan inhibition of TGFβ superfamily ligands that signal through

the ActRIIB receptor.

CHAPTER 1. INTRODUCTION

1.1   Objectives

The purpose of our studies is to determine the role of TGFβ superfamily signaling in

NASH pathology, with specific focus on liver and muscle cross-organ relationships

involved in concomitant muscle atrophy observed in patients. While data has been

generated that demonstrates the importance of TGFβ/Smad signaling in liver disease and

muscle atrophy separately, limited evidence exists that highlights the commonalities of

TGFβ signaling in both tissues. Furthermore, the impact of sarcopenia on health and

prognosis of liver disease (including NASH) patients is a burgeoning field that carries

great promise for novel therapeutic options to better treat those stricken with such

diseases. We postulate that understanding the elements involved in liver disease that

result in sarcopenia is an opportunity to explore an endocrine relationship that has novel

implications on diseases with large unmet medical need.

The central hypothesis of this thesis is that TGFβ factors modulate NASH progression

and directly initiate muscle atrophy programs which are responsible for concomitant

sarcopenia.

To test this hypothesis, we defined the following objectives:

1. Evaluate and characterize a 2-hit *in vivo* model of NASH

2. Determine whether TGFβ superfamily signaling plays a role in NASH disease

progression *in vivo* and whether those effects can be recapitulated *in vitro*

The outcome of this proposal could potentially identify a novel endocrine relationship between liver and muscle that contributes to the concomitant muscle atrophy accompanied with end-stage liver diseases. Furthermore, inhibition of these hepatic-based factors defining the molecular underpinnings of the endocrine relationship could provide substrate for seminal targets for a disease with large unmet medical need.

1.2 Organization

In order to better help familiarize the reader to the field of TGFβ signaling in liver and muscle biology, this thesis consists of a literature review (Chapter 2), with particular emphasis on liver regeneration and muscle atrophy. Also in Chapter 2, there is a literature review on NASH and related liver diseases with particular emphasis on the impact those disease have on muscle atrophy. Chapter 3 describes the materials and methods used in the research. Experimental results collected throughout our research are presented in Chapter 4. Discussion of the impacts of our findings, and potential future efforts are presented in the discussion section (Chapter 5).

CHAPTER 2. LITERATURE REVIEW

2.1   Etiology of liver disease

The liver plays a vital role in regulating many of the nutrient constituents found in blood such as glucose, protein and fat. In addition, the liver also serves as the master "detoxifier" of the body by cleansing the system of many harmful substances as well as removing old, worn out red blood cells. As a result of its perpetual exposure to a multitude of both natural and synthetic chemicals, the liver is subjected and susceptible to constant injury and the need for rapid repair. If left uncorrected, chronic liver injury eventually leads to the development of liver fibrosis. Liver fibrosis is a multi-cellular process that is highly conserved and specifically well-coordinated. In the early stages of liver injury and cell death, liver cells or hepatocytes, are quickly surrounded by infiltrating immune cells that can produce cell activating substances. These substances are comprised of reactive oxygen species and inflammatory cytokines leading to the activation of perivascular hepatic stellate cells (HSCs) (Safadi and Friedman, 2002). HSCs work closely with injured and uninjured hepatocytes, hepatic macrophages (Kupffer cells) cholangiocytes, endothelial cells and infiltrating immune cells in orchestrating the fibrotic response (Seki et al., 2015). Initially, activated HSCs generate plenteous amounts of abnormal extracellular matrix components (consisting of collagen, other glycoproteins, and glycans), resulting in a temporary scar at the site of injury protecting the liver from incurring any additional damage by providing mechanical and architectural support (Yin et al., 2013). However, when the liver is under constant injury and remodeling, a maladaptation of regeneration occurs leading to decompensated state

resulting in excessive agglomeration of ECM negatively affected liver dysfunction, most notably liver fibrosis. The key environmental influences that lead to liver fibrosis include chronic alcohol abuse, virus C infection and a diet composed of high fat and cholesterol can promote liver fibrosis and the eventual development of cirrhosis (Bataller et al., 2005).

2.2 NASH

Nonalcoholic fatty liver disease (NAFLD), a precursor to nonalcoholic steatohepatitis (NASH), is the most common cause of liver disease in the world, affecting nearly 30% of individuals. Due to its strong relationship to obesity and metabolic disorders, NAFLD is considered the hepatic manifestation of metabolic syndrome. Concordant with increasing global rates of obesity, the prevalence of NAFLD patients have been increasing, and are projected to continue rising for the foreseeable future (Dowman, Tomlinson, & Newsome, 2011). NAFLD's pathology is defined by the excessive accumulation of lipids (in the form of triglycerides) in the liver in the absence of excessive alcohol intake. In some cases, NAFLD may advance into the more aggressive form of liver disease, NASH. In addition to the primary steatosis, characteristic pathology of NASH includes the essential hallmarks of disease such as hepatocyte injury, inflammation, and fibrosis. NASH can progress into liver cirrhosis and hepatocellular carcinoma (HCC), requiring liver transplantation (MacHado & Diehl, 2016). By 2020, it is projected that NASH will be the leading cause of liver transplants in the United States (Kneeman, Misdraji, & Corey, 2012).

Disease progression in NASH is not fully understood, but is believed to encapsulate multiple stages of injury, or "hits", that accumulate in the liver. Tilg and Moschen proposed the parallel multiple hit hypothesis that outlined a complicated interplay between a number of parallel hits (e.g. disrupted lipid metabolism, lipotoxicity, oxidative stress, mitochondrial dysfunction, ER stress, gut derived endotoxins, altered cytokines and adipokines, and genetic predisposition) (Tilg & Moschen, 2010). Although the pathology of NASH is not linear, it can be visualized in a way that outlines the progressive severity of the disease (Figure 2.1).
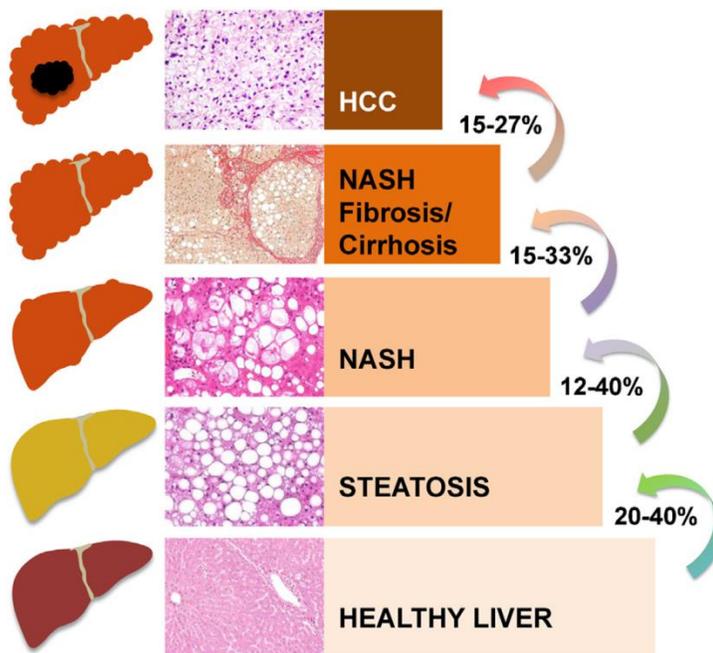
Figure 2.1 Disease progression of a healthy liver through NAFLD, NASH, and HCC.

Although significant progress has been made in the diagnosis, there is still debate surrounding a more accurate and exact diagnosis for NASH. Standard diagnosis, entails the use of liver biopsies to assess the degree and presence of steatosis, lobular

inflammation, hepatocellular ballooning, perisinusoidal fibrosis, hepatocellular glyocgenated nuclei, lipogranulomas, acidophil bodies, fat cysts, Mallory bodies, iron deposition, and megamitochondria. Although it is not considered to be mandatory for a NASH diagnosis, fibrosis is considered to be one of the most important pathologies in determining severity of the disease and its potential progression (Dowman et al., 2011).

2.3 Liver and muscle

The liver and the skeletal muscle system have a well-established interdependent endocrinological connection in both normal physiological and pathological states. For example, in normal physiological states, these two organs equally contribute to the maintenance of glucose homeostasis by storage and metabolic mechanisms. Conversely, this interdependent relationship has been highlighted in more pathological states and continues to be expounded on in both clinical and preclinical settings. Clinically, patients with liver cirrhosis exhibit irregularities in their ability to store glucose as glycogen in skeletal muscle (Kruszynska et al., 1988). Furthermore, muscle wasting or sarcopenia is a common and frequently disregarded comorbidity that adversely affects quality of life, and even recovery from surgery or even infection (Montano-Loza et al., 2014).

This severe mode of muscle wasting has generally been found to be an effective predictor for mortality in a multitude of diseases. Patients with cirrhotic livers and contemporaneous muscle atrophy tend to have lower survival rates and more complications post-liver transplant. Paradoxically, most complications in liver cirrhosis patients resolve following a successful transplant, except for the underlying muscle wasting which in some incidents may actually worsen (Dasarathy et al., 2016). In a cross

sectional Korean study, subjects with radiological evidence of hepatic steatosis has a

greater decrement in appendicular muscle mass (determined by bioelectrical impedance)

as the NAFLD activity score increased (Koo et al., 2016). Moreover, even muscle

function may also provide clinical utility. There is now evidence that demonstrates the

value of reversing muscle loss in cirrhotic patients may be beneficial. This was

underscored in a study where men treated with testosterone who were diagnosed with

cirrhosis of the liver and low serum testosterone was able to safely promote muscle mass,

bone mass and hemoglobin, while in parallel reduce fat mass and HbA1c (Sinclair et al.,

2016). Studies are ongoing to verify the value of increasing muscle mass and the long

term consequences on survival.

It is of paramount importance to further the understanding and characterize the systemic

cues that initiate these sequences of events. It has been proposed that members of the

TGFβ family play integral roles in moderating the growth and disease states of both liver

and skeletal muscles while certain members may serve as a nexus between the two organs

(Tsuchida, 2004). Nonetheless, it is imperative to ascertain which specific TGFβ

members are involved in the cross-talk between the two organs.

2.4   TGFβ signaling

The transforming growth factor-β (TGFβ) superfamily is an ever evolving and

unremittingly expanding group of factors, comprised of 33 genes encoding for

polypeptides that exist as either homo or heterodimers. The members of the superfamily

include bone morphogenetic proteins (BMPs), growth and differentiation factors (GDFs),

Activins (ACTs), Inhibins (INHs), and glial-derived neurotrophic factors (GDNFs), as

well as some proteins not included in the above families, such as Müllerian inhibiting substance (MIS), also known as anti-Müllerian hormone (AMH), left-right determination factor (Lefty), and nodal growth differentiation factor (Nodal) (Figure 2.2) (Poniatowski et al., 2015). TGFβ superfamily ligands trigger their downstream effects via interactions with the extracellular domains of specific type II receptors (e.g. TGFBR2, ACTRIIA, ACTRIIB, BMPR2 etc.) consequently inducing a conformation change. The conformational shift enables the recruitment and phosphorylation of their respective type I receptor and their intracellular serine residues through its serine/threonine kinase domain. There are seven known type I transmembrane receptors identified as Activin receptor-like kinases (ALK1-7). Activation of the type I receptor initiates an intracellular signaling cascade through the carboxy-terminal phosphorylation of a set of receptor regulated transcription factors known as Smads or R-Smads. The activated R-Smads will then form an olgiomeric complex with a co-Smad and traverse into the nucleus to where it transduces extracellular signaling by modifying specific target gene expression (Lagna et al. 1996; Zhang et al. 1996; Kawabata et al. 1998).

Generally in most cell contexts, Activins and TGFβs will induce the phosphorylation of R-Smad2 and Smad3, while BMPs will employee the R-Smad1, Smad5, and Smad8 transcription factors for their transduction. The TGFβ superfamily members and their downstream signaling are both highly conserved throughout species and are implicated in numerous physiological processes that include cellular proliferation, inflammation, body mass control, tissue healing, epithelial–mesenchymal transition (EMT), and extracellular matrix (ECM) remodeling (Akhurst & Hata, 2012). The TGFβ family requires a high

level of precision in the balance of activity and expression to preserve tissue integrity and anomalies in this regulation can contribute to the pathogenesis of the sequelae stated above.
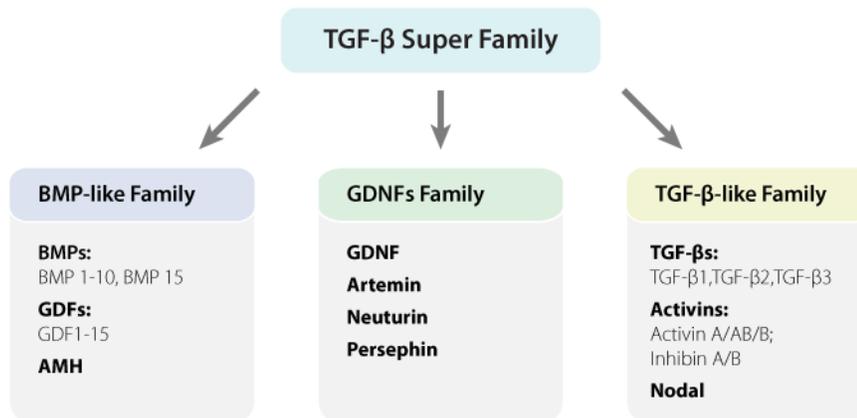
Figure 2.2 The TGFβ superfamily.

2.5   TGFβ signaling in liver biology

Liver has a remarkable ability to regenerate following injury and partial hepatectomy (up to 70%) (Fausto et al, 2006; Michalopoulos, 2007). Following development, the liver maintains a residential progenitor cell population that inhabits areas in the portal triad. Upon activation, these unique cells give rise to nascent hepatocytes (Fougere-Deschatrette et al, 2006; Oertel & Shafritz, 2008, Font-Burgada J et al., 2015) (Figure 2.3). The liver's unique ability to preserve its size and mass in spite of constant damage and ongoing repair necessitates well-orchestrated processes that are stringently regulated and controlled by these cells. Aberrant coordination of these regenerative processes is evident in liver fibrosis leading to scarring (cirrhosis) and eventual liver failure. The

TGFβ superfamily plays a definable role in maintaining liver homeostasis and has been revealed that disruption in its signaling and expression can afflict the liver resulting in several diseases such as NASH, hepatocellular carcinoma (HCC) and cirrhosis. Activin and Inhibin proteins are members of the TGFβ superfamily, that have been described as potent regulators of inflammation and differentiation of many cell types found in the liver. More specifically, Activin A has been described as a versatile cytokine and a major culprit in promoting hepatic inflammation, fibrosis and remodeling. Higher levels of Activin A protein have been observed in fibrotic livers. These findings have also translated over to humans where increased serum Activin A levels were found in NASH patients when compared to obese or lean controls (Polyzos et al., 2016). Although the mechanisms have not been fully explained, Activin A has been implicated in the manifestation of the liver fibrosis through its reported production of collagen and TGFβ1. Additionally, in liver precursor and HSCs, Activin A increases the stimulation of a key regulator of ECM deposition known as connective tissue growth factor (CTGF) (Ding et al., 2016).
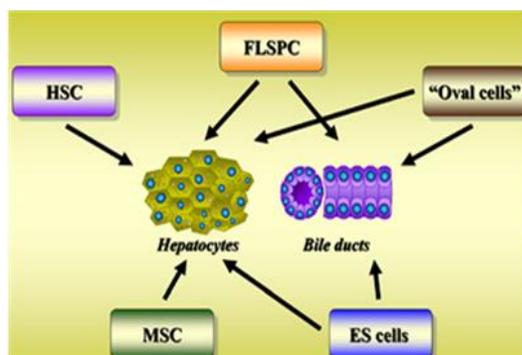
Figure 2.3 HSC-Hematopoietic stem cells, FLSPC-fetal liver stem/progenitor cells, MSC-mesenchymal stem cells, and ES-embryonic stem cells.

Activin A also plays a significant role in cellular division and death. Activin A simultaneously inhibits proliferation and induces apoptosis of hepatocytes which may assist in the cessation or final stages of liver regeneration. Similar to hepatocytes, progenitor cell activation and subsequent replication may also be mediated by the presence of Activin A. The anti-mitogenic effect of Activin A has been corroborated, both *in vitro* and *in vivo* (Hully et al, 1994; Schwall et al, 1993). The *in vitro* validation and mechanism has been delineated in several studies. In one study, a simple experiment was conducting measuring the effects of Activin A on epidermal growth factor (EGF)-induced DNA synthesis in cultured rat hepatocytes. Hepatocyte DNA synthesis was blocked by the presence of Activin A overcoming the up regulation and proliferative effects of Follistatin generated by EGF (Niimi et al, 2002). Complementary, in the highly proliferative hepatoma cell line HepG2 cells, one group demonstrated Activin A via Smad2 nuclear translocation induced apoptosis comparatively to that of TGFβ. This effect could then be ablated by blocking the downstream propagation of Activin receptor IIB activation using a dominant negative approach. (Wei Chen et al., 2000).

Small hepatocytes are a subpopulation of liver cells that have a high propensity for growth and the ability to differentiate into mature hepatocytes supporting growth and homeostasis. Inhibition of the Activin natural antagonist Follistatin with an inhibiting antibody resulted in suppression of DNA synthesis in small hepatocytes presumably through the increasing the bioavailability of Activin A and presumably Activin B (Ooe et al, 2012).

This claim continues to be substantiated in studies monitoring hepatic oval cell proliferation. Oval cells may also play a critical function as facultative liver stem cells. Exogenous Activin A treatment on an oval cell line (LE6) robustly inhibited proliferation in a dose dependent manner by down regulating cyclin E and cyclin D1 while increasing cyclin dependent kinases p15^{INK4B} and p21^{WAF1}. This effect was then reversed by the co-incubation of Follistatin protein (Chen et al., 2014).

In vivo animal models that demand high levels hepatocyte proliferation such as partial hepatectomy Activin A mRNA levels have been shown to rapidly decrease within 12 hours following surgery (Gold et al, 2005). Once cellular division has reached the proper threshold, it will cease and Activin A levels will rise to assist in the completion of regeneration and restore liver micro-architecture by stimulating tubulogenesis of sinusoidal endothelial cells and collagen production by hepatic stellate cells (Endo et al, 2004; Wada et al, 2004). Follistatin has been shown to reverse many of the effects presumably elicited by Activin A. In model, a single intraportal administration of Follistatin accelerated liver regeneration by amplifying the initial bout of DNA synthesis as confirmed by bromodeoxyuridine (BrdU) labeling (Kogure et al, 1995). However, if continued treatment of Follistatin persists then, liver architecture may not be restored to its fully functional state.

In an animal model that reflects aggressive liver fibrosis, treatment of Follistatin has been found to ameliorate the histopathological signature of this disease (Endo et al, 2006; Patella et al, 2006). In this model, liver fibrosis was induced with chronic CCl_4

administration and rats were concurrently administered recombinant Follistatin protein. Follistatin treated rats had significantly less alpha-smooth muscle actin staining, TUNEL-positive cells and hepatic hydroxyproline content indicative of attenuated fibrosis. The efficacy produced by Follistatin presumably would be attributed mostly to inhibition of Activin A, as blocking its activity with a selective antibody protects the liver from CCl_4 induced injury (Wang et al, 2013). These data also correlate to the human studies described earlier with the positive correlation of Activin A expression and severity of liver disease.

Along the same vein as liver disease, the natural process of aging presents an additional problem, due to the progressive loss in liver plasticity and a attenuated proliferative response leading to a deficiency in complete regeneration (Timchenko, 2009). Preclinically this regenerative inadequacy has been ascribed to concomitant age dependent increases in hepatic Activin A levels, as livers of older rodents (greater than 19 months) and older individuals (greater than 65 years of age) (Menthena et al, 2011) displayed increased transcript and protein expression levels. Rats as early as two months old were found to have higher levels of Activin A protein that continued to rise until they reached 19 months of age. Analogous to the above-mentioned study, Activin A was also discovered to increase a cyclin dependent kinase inhibitor, p15INK4b, which may be responsible for driving cells into quiescence and may eventually lead them to senescence. Increased sensitivity to Activin signaling in aged rats was also found as denoted by the reduction in Ki-67 positive cells. Correspondingly, these findings display a level of congruence imparting higher confidence in their ability to translate to human disease.

2.6   TGFβ signaling in skeletal muscle biology

TGFβ family members have been implicated in both homeostasis and disease, but only limited members have been studied in skeletal muscle. In this outline we will review the current findings of the two key members (Activin A and Gdf8) of the TGFβ family along with a natural antagonist (Follistatin) and their role in muscle.

Myostatin, or growth and differentiation factor-8 (Gdf8), is a well know member of the TGFβ superfamily. While a number of TGFβ members have been shown to influence muscle growth, Gdf8 is considered one of the more dominant negative regulators of skeletal muscle mass that is extensively conserved throughout the mammalian species. It is operative during development and adulthood and these roles have been heavily examined since its advent. Gdf8 precursor protein is secreted in an unprocessed pro-form. The mature form of Gdf8 is derived from the proteolytic processing of its precursor. This process of activating of myostatin is facilitated through the cleavage of the propeptide by the bone morphogenetic protein (BMP)-1/tolloid family of metalloproteinases (Elkina, von Haehling, Anker, & Springer, 2011,and Szláma, Trexler, & Patthy, 2013). Activated Gdf8 will then bind to its primary cognate receptor, Activin IIB receptor (ActRIIB), or in some cases even Activin IIA receptor (ActRIIA) (Gilson et al, 2009; Huet et al, 2001; Sako et al., 2010). Once bound, Gdf8 will elicit a cascade of events that lead to the translocation of regulatory Smads 2/3 to the nucleus and alteration of gene expression (Han et al, 2007; Welle, 2009) (Figure 2.2). The Gdf8 mediated gene response is the primary suppressor on the activation of skeletal muscle satellite cells and disrupting the balance of protein synthesis/degradation. Gdf8 has been shown to be an anti-

proliferative agent in satellite cell expansion by the strict modulation of Pax7 and Myod1 gene expression in conjunction with cell cycle control factors (McCroskery et al, 2003; McFarlane et al, 2008).

In terms of protein metabolism and muscle growth, Gdf8 is culpable for the down-regulation of the Akt/mTOR signaling pathway, as evidenced by the decreased phosphorylation of AKT. The Akt/mTOR pathway is the main driver in promoting skeletal muscle anabolism and it down regulation is responsible for skeletal muscle atrophy (Rodriquez et al., 2014). In summary, dysregulation of Gdf8 can affect both skeletal muscle plasticity and hypertrophy.

It has been well documented that neutralization, reduction or deletion of gene expression will have profound effects on stimulating muscle growth. Several laboratories and pharmaceutical companies have developed a multitude of methods that impede Gdf8 signaling such as neutralizing antibodies, natural protein inhibitors, siRNA and even gene therapies. Innumerable preclinical studies have provided evidence that inhibition of Gdf8 can improve both muscle mass and strength in multiple disease states. For instance, tumor bearing cachectic (C26 colon adenocarcinoma and PC3 prostate carcinoma) mice treated with a Gdf8 neutralizing antibody was able to significantly preserve muscle mass and strength (Smith et al., 2015). Additionally, in aged mice (22 months), 4 weeks of Gdf8 antibody treatment demonstrated a 7% increase in lean body mass and a 20% increase in grip strength improving both quality and quantity of muscle. Unexpectedly, these studies revealed that Gdf8 inhibition also provided a modest improvement in insulin

sensitivity (Camporez et al., 2016). This augmentation of skeletal muscle metabolism and insulin sensitization was also substantiated in another study where reductions in Gdf8 mRNA increased glucose uptake in type 1 diabetic (Akita) mice by upregulating glucose transporters Glut1 and Glut4 (Coleman et al., 2016). These therapeutic modalities have clearly demonstrated the potential clinical utility for a myriad of muscle and metabolic disorders (Bogdanovich et al, 2005; Murphy et al, 2011; Tsuchida 2008; Wagner et al, 2002).
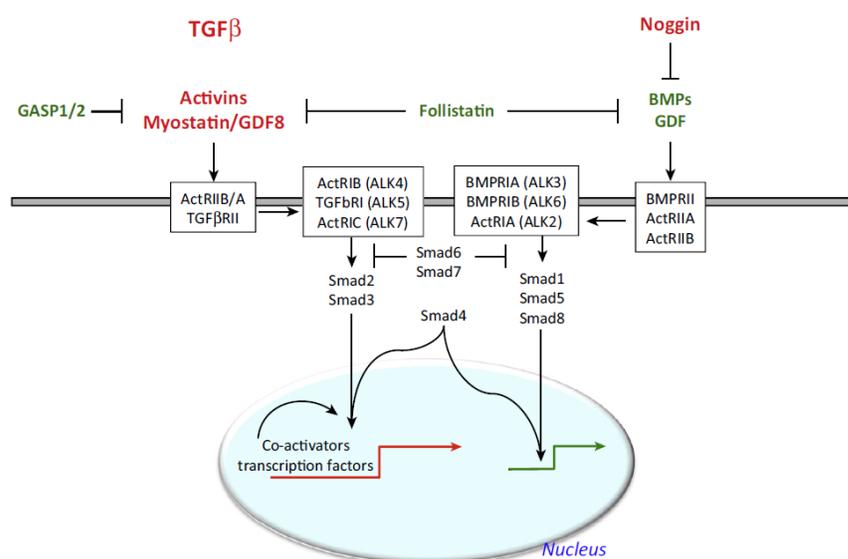
Figure 2.4 Cross-talk between myostatin/Activin A and BMP signaling in skeletal muscle. **Sartori,** *Trends in Endocrinology and Metabolism September 2014.*

More recently, studies have uncovered other TGFβ members as intermediaries of skeletal muscle physiology. One group found that a Follistatin transgenic mouse produced a robust muscle hypertrophy phenotype greater than what had been observed by myostatin

deletion (Lee, 2007). These findings suggest additional TGFβ members can modulate muscle growth and development.

Empirical confirmation of these data was seen in an experiment by Lee *et al.*, where Gdf8 null mice were crossed with mice carrying a Follistatin transgene (Lee, 2007). These mice exhibited extreme muscle growth when compared to the Gdf8 null mice, reaffirming the existence of other regulators of muscle mass. An experiment utilizing another broad inhibitor of the TGFβ superfamily, ActRIIB-Fc (engineered molecule that fuses the ECD of Activin receptor IIB to an Fc domain of IgG1), also produced similar results. Treatment with the ActRIIB-Fc decoy receptor in a Gdf8 null background produced additional gains in muscle mass reiterating that the presence of other regulators specifically signal through the ActRIIB receptor (Lee et al, 2005). Follistatin is a natural antagonist to several members of the TGFβ pathway including both Gdf8 and Activins A and B. Akin to FST; ActRIIB-Fc also binds many of the same members providing a focused substrate in identifying the additional muscle regulators modifying skeletal muscle.

Predicated on these data, Activin A appears to be the most likely suspect affiliated with muscle. Activin A belongs to the Activin subgroup of the TGFβ family, which is comprised of many members that are formed through the dimerization of the following four subunits: βA, βB, βC, and βE (Carney et al, 2011; Mellor et al, 2003; Mellor et al, 2000). The Activin A protein complex is comprised of a disulphide-linked homodimer containing two of the aforementioned βA-subunits. Similar to Gdf8, once Activin A is

processed and secreted, it can elicit a Smad based gene response by binding to its respective receptors, ActRIIA and IIB.

Activin A has been linked to etiologies of multiple diseases ranging from cancer metastasis to osteoporosis (Fajardo et al, 2010; Leto, 2010; Leto et al, 2006; Lotinun et al, 2010; Terpos et al, 2012). Activin A shares some functional overlap with Gdf8 in terms of skeletal muscle as illustrated by He *et al*. Studies from this group demonstrated that muscle precursor cells treated with Activin A blocked the expression of the two key myogenic transcription factors, Pax7 and Myod1, resulting in a loss of activation and differentiation much akin to Gdf8 (He et al, 2005; Wagner, 1993). Effects of Activin A on satellite precursor cells were also supported by data generated by Yaden et al., where it was ascertained that the inhibition of Activin A lead to an increase of Pax7 positive cells in a model of muscle injury and regeneration. In the article, local exposure of normal muscle to Activin A was shown to reduce myofiber diameter and activate myocellular degeneration through the concordant activation of inflammation and the induction of muscle atrophy via E3 ligases (Yaden et al., 2014). Another group expounded on this finding and showed that Activin A stimulated muscle catabolism both in C_2C_{12} myotubes and mice and was solely dependent on p38β MAPK signaling (Ding et al., 2016). Lastly, elevated systemic levels of Activin A have been shown to engender a phenotype reminiscent of severe cachexia by engaging in the myostatin pathway (Chen et al., 2014).

To conclude, studies need to investigate the relevance of Activin A and Gdf8 along with additional TGFβ members and define their overall contribution to liver disease and the concurrent muscle atrophy.

CHAPTER 3. MATERIALS AND METHODS

3.1 Animal care and use

All mouse experiments were performed with the approval of Eli Lilly and Company's

Institutional Animal Care and Use Committee and are in accordance with the National

Institute of Health Guide for the Care and Use of Laboratory Animals.

For diet-induced obesity (DIO) studies, male C57BL/6 male mice were used (Jackson

Laboratories, Bar Harbor, ME). DIO animals were placed on a high-fat diet (Research

Diets, New Brunswick, NJ) with 60% kcal from fat at 6 weeks of age, and purchased 14

weeks later. Age-matched control animals were fed standard chow (TD 5001 with 0.95%

calcium and 0.67% phosphorus, Teklad, Madison, WI) for the same period of time.

Animals were acclimated for 2 weeks in a temperature controlled room ($(22\pm2°C)$, and a

12:12 hour light-dark cycle (lights on at 6:00 am) with ad lib access to food and water

prior to beginning of study. Mice were then randomized into treatment and control groups

according to body weight prior to the beginning of the study.

3.2 Carbon tetrachloride (CCl_4) induced liver injury

For longterm studies hepatic fibrosis was induced by intraperitoneal (IP) injections of 1:5

dilution of CCl_4 (Sigma Aldrich) in corn oil (1 ml/kg) twice weekly for 1 or 4 weeks. The

mice in normal control groups received only corn oil injections for the duration of the

study in the same dosing regimen of CCl_4. For acute studies, animals received a single

dose of CCl_4. Twenty four hours after the final administration of CCl_4, animals were

anesthetized with isoflurane, and blood was collected via cardiac puncture before

secondary euthanasia by means of cervical dislocation. Following secondary euthanasia, liver and muscles were excised, weighed, and snap frozen in liquid nitrogen. Tissue and serum samples were kept frozen at -80 °C until analyzed.

3.3 Combination of CCl$_4$ injury and DIO model

Hepatic injury was induced as described above. Animals were provided ad lib access to high fat chow for at least 22 weeks prior to start of study and high fat feeding was maintained throughout the experiment.

3.4 Bile duct ligation

Bile duct ligation studies were performed as previously described (Tag et al., 2015) in male Sprague Dawley rats. Animals were sacrificed as previously described 3 hours, 6 hours, 12 hours, 24 hours, 4 days, 6 days, 11 days, and 15 days after surgery.

3.5 Inhibition of TGFβ family members

TGFβ family members were inhibited *in vivo* using antibody therapies dosed at 10 mg/kg 24 hours prior to CCl$_4$ administration. Anti-Gdf8 and anti-Activin A antibodies were obtained from Eli Lilly and Company (Indianapolis, IN), and Actr2b-Fc antibody was obtained from Acceleron Pharma (Cambridge, MA).

3.6   Body composition (quantitative NMR)

Lean body mass, fat mass, and free water content were measured using nuclear magnetic

resonance once weekly throughout the studies (NMR; Echo Medical systems, Houston,

TX).

3.7   Biochemical assays

Blood was collected via cardiac puncture 24 hours after the final CCl_4 administration, and

serum was separated using Multivette 600 Z-Gel serum separating tubes (Sarstedt,

Nümbrecht, Germany). Serum aspartate aminotransferase (AST), alanine

aminotransferase (ALT), glucose, and total bilirubin (T-Bil) were assayed with a Hitachi

Modular Analyzer (Roche Diagnostics, Indianapolis, IN).

Serum FGF21 and CD14 protein content was assayed via ELISA kits provided by R&D

systems (MF2100 and MC140, respectively). Hepatic FGF21 was quantified using the

same ELISA kit. Serum Activin B protein content was analyzed via ELISA kit (Ansh

Labs, Webster, TX).

Serum Activin A protein was assayed after samples underwent treatment with 10mM

DTT in PBS for 1 hour at room temperature prior to plating. The antibody was coated

and was reconstituted in PBS to a final concentration of 100 µg/mL (R&D Systems

#AF338, Minneapolis, MN). One hundred microliters per well of antibody were diluted

to 1 µg/mL in coating buffer (Hyclone SH30256.01, Waltham, MA), incubated 1 hour at

37°C, blocked for 1 hour, then samples were incubated at room temperature for 1 hour.

Poly streptavidin-HRP and TMB block steps were performed and plates were read at

450-630 nM. The ELISA was validated using purified Activin A protein.

3.8 Histology

Liver and muscle tissues were processed and embedded in paraffin using standard

methods. Histology was evaluated using hematoxylin and eosin (H&E) staining and

Mason's trichrome staining at 5μm. Liver sections were stained using a trichrome

staining kit purchased from Abcam (Cambridge, MA). Hydrated slides to water and place

in Bouin's fixative for 1 hour at 56°C in a preheated dish or jar. Samples were then

placed Bouin's fixative overnight at room temperature. Sections were rinsed in distilled

water and placed in Weigert's iron hematoxylin solution for 10 minutes. Samples were

washed in running tap water for 10 minutes then placed in Biebrich scarlet-acid fuchin

solution for 17 minutes. Samples were then rinsed and placed in phosphomolybdic-

phosphotungstic acid solution for 10-15 minutes. Sections were transferred directly to the

aniline blue solution for 20 minutes. Sections rinsed in distilled water and dehydrate,

clear in xylene, and then cover-slipped, using a synthetic mounting medium.

For each muscle, the distribution of the fiber diameter was calculated by analyzing 100 to

150 myofibers. Images were acquired using digital slide scanning (ScanScope XT,

Aperio, Vista, CA).

3.9 Quantitative real-time PCR

mRNA analysis of liver and muscle was performed via qRT-PCR on RNA extracted from

tissues using TRIzol reagent and the PerfectPure RNA 96 CellVac Kit (5 PRIME,

Germany). RNA purity was calculated using absorbance at 260/280 nm quantified via

Nanodrop (ThermoFisher Scientific, Wilmington, DE). 2 µg of extracted RNA was

reverse transcribed using a MultiScribe MuLV high capacity cDNA reverse transcription

kit (ThermoFisher Scientific, Wilmington, DE) in a 50µL reaction. The resulting cDNA

was combined with TaqMan Fast Universal Master Mix (ThermoFisher Scientific,

Wilmington DE) and specific primer probes (see primerprobe ID on table below) for

qPCR analysis on the Applied Biosystems 7900HT Fast System (ThermoFisher

Scientific, Wilmington DE) for 40 cycles in a 10µL reaction. All CT values were

normalized to GAPDH gene for normalization.

Table 3.1 Taqman primer probe ID numbers for genes used in mRNA expression analysis.

Gene	Probe ID
Gapdh	Mm99999915_g1
Inhba	Mm00434339_m1
Inhbb	Mm03023992_m1
Gdf8	Mm01254559_m1
Gdf15	Mm00442228_m1
Trim63	Mm01185221_m1
Fbxo32	Mm00499523_m1

3.10 *In vitro* experiments

In vitro experiments were performed using primary hepatocytes isolated as previously

described (Berry, M. N. and Friend, D. S. 1969) and C2C12 myoblasts were obtained

from ATCC (Manassas, VA). Myoblasts were differentiated in growth media

supplemented with 2% horse serum for 5 days with daily media change. Hepatoxins were administered directly onto hepatocyte media for 24 hours prior to media collection. Unless noted otherwise, CCl_4 was administered at 0.5%/volume. Collected hepatocyte media was diluted 1:10 in myoblast differentiation media before addition to C2C12 cells. After 5 days, muscle cells were imaged and diameter quantified using Aperio ImageScope software. Cell media aspartate aminotransferase (AST), alanine aminotransferase (ALT), glucose, and total bilirubin (T-Bil) were assayed with a Hitachi Modular Analyzer (Roche Diagnostics, Indianapolis, IN). Hepatocyte media FGF21 was analyzed by ELISA kit listed above.

3.11 Data analysis

All data are expressed as the mean ±SEM. Statistical analysis was conducted using GraphPad Prism version 7. Statistical significance (p-value ≤0.05) was analyzed by one-way ANOVA.

CHAPTER 4. RESULTS

4.1 Characterization of two-hit NASH model

We evaluated an *in vivo* model of non-alcoholic steatohepatitis (NASH) to better understand the mechanisms of disease progression both in the liver and the concomitant muscle atrophy (Kubota et al., 2013). Animals were separated into 8 different groups based on diet, duration of time on study, and CCl_4 administration (Table 4.1).

Table 4.1 Groups in two-hit *in vivo* NASH study.

Group Number	Obesity State	Hepatotoxin	Time on Study
1	Lean	Corn Oil	1 Week
2	Lean	CCl_4	1 Week
3	DIO	Corn Oil	1 Week
4	DIO	CCl_4	1 Week
5	Lean	Corn Oil	4 Weeks
6	Lean	CCl_4	4 Weeks
7	DIO	Corn Oil	4 Weeks
8	DIO	CCl_4	4 Weeks

Due to the hepatotoxic and pro-fibrotic effects of CCl_4 (Weber, Boll, & Stampfl, 2003), we anticipated that characteristic markers of liver injury would be increased following administration. To investigate these effects, lean animals that were on a standard chow diet (SD) or diet induced obese (DIO) animals fed a high fat diet were injected with CCl_4 intraperitoneally twice weekly (q.a.d.) for one week while another cohort remained on the study for 4 weeks. Twenty four hours after the last CCl_4 injection, muscle, liver, and

blood was collected and the serum was analyzed biochemically for markers of hepatic injury. A shorter timecourse was chosen to assess known liver injury responses to CCl_4 that peak roughly 72 hours after injury. The 4 week timepoint replicates the published study design, and theoretically provides more time for disease pathology to manifest. At both timepoints, aspartate aminotransferase (AST) and alanine aminotransferase (ALT) were dramatically increased in both groups injected with CCl_4 (Figure 4.1). Despite their significant obesity, the DIO animals, without CCl_4 injury, did not have elevated serum ALT or AST levels compared to their lean controls. After 4 weeks of injury, animals started to show signs of liver failure (as determined by diminished hepatic gluconeogenesis, bilirubin processing, and histopathological features) which likely caused ALT/AST increases to be less responsive to CCl_4. Despite this effect, AST levels in the DIO+CCl_4 combination group exhibited greater AST levels than lean+CCl_4 controls suggesting enhanced disease progression in the DIO+CCl_4 animals.
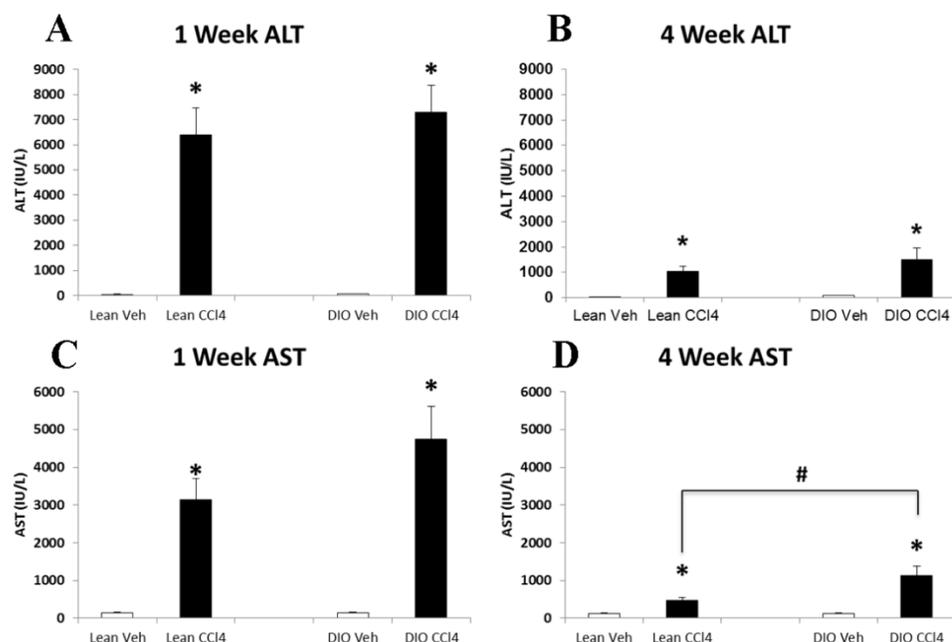
Figure 4.1 Biochemical assessment of the two hit model. DIO male C57BL/6 mice were chronically administered CCl$_4$ for either 1 or 4 weeks. Male C57BL/6 serum was collected via cardiac puncture 24 hours after the final CCl$_4$ injection. After 2 injections, ALT **(A)** and AST **(C)** were increased in circulation independent of diet. After 4 weeks of biweekly CCl$_4$ injections, ALT **(B)** and AST **(D)** levels were increased compared to corn oil controls, but the magnitude of the increase was blunted. At this timepoint, the combination of DIO+CCl$_4$ exhibited significantly increased AST levels compared to those of lean CCL$_4$ controls. Data are expressed as means ± S.E.M. of 5 mice per group. Significance is indicated *P ≤ 0.05 (Dunnett's one-way ANOVA).

While there is some evidence that increased hepatocellular triglycerides may protect against liver injury acutely (Cusi, 2012), the histology suggests diminished liver triglycerides at the later timepoint, and the indications of liver failure (Figure 4.2) are a result of a pronounced liver pathology after 4 weeks of insult. Increased total bilirubin and reduced hepatic gluconeogenesis after 4 weeks was only observed in the DIO+CCl$_4$ cohort. This reduced hepatic function along with increased ALT/AST levels is suggestive of a natural proclivity to greater injury due to residual adiposity in these animals.
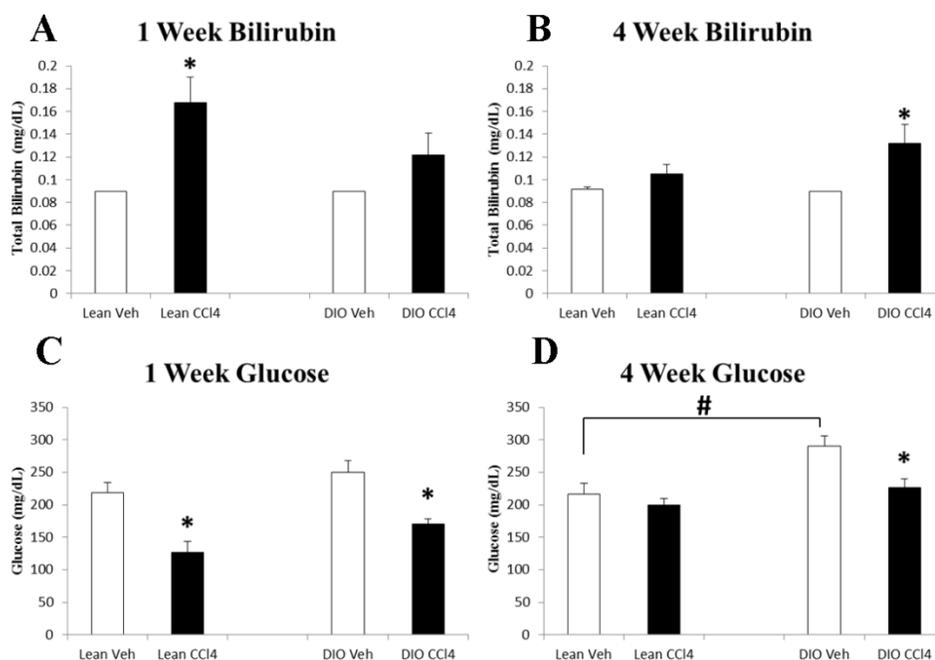
Figure 4.2 Functional assessment of the two hit NASH model. DIO male C57BL/6 mice were chronically administered CCl$_4$ for either 1 or 4 weeks. At the end of the studies, serum levels of bilirubin (**A & B**) and glucose (**C & D**) were measured as indicators of liver injury and function. Data are expressed as means ± S.E.M. of 5 mice per group. Significance is indicated *P $\leq$ 0.05 compared to corn oil control P $\leq$ 0.05 (Dunnett's one-way ANOVA).

The two-hit model of NASH was chosen in order to emulate both the peripheral characteristics of metabolic disorder along with the hepatic damage associated with fibrosis as a result of chronic injury (Buzzetti, Pinzani, & Tsochatzis, 2016).

In order to assess the presence of standard pathological features of NASH development in the liver, hemotoxylin and eosin (H&E) staining was performed. Lean mice fed standard chow diet (SD) with no injury lacked any abnormal features, while DIO mice without injury exhibited abundant steatosis (the hepatocellular storage of lipid droplets), especially near zone 3 (Figure 4.3). NAFLD and NASH involve a multitude of

pathologies associated with obesity and metabolic syndrome including an increase in circulating pro-inflammatory milieu, insulin resistance, and increased free fatty acids (FFA) which result in altered glucose and lipid metabolism that drive lipid accumulation in the hepatocytes (Rinella, 2015). Independent of CCl_4 administration, DIO animals showed significant steatosis, while SD animals showed little to no steatosis at either time point (Figure 4.3). Interestingly, steatosis was reduced after 8 injections of CCl_4 along with high fat feeding. This finding was consistent with previous studies (Kubota et al., 2013). Such a reduction in steatosis can most likely be attributed to the overall body weight loss related to malnutrition exhibited by these animals reminiscent of high risk patients during end stage liver disease (Bambha, Dodge, Gralla, Sprague, & Biggins, 2015). Additionally, as end stage liver disease progresses, there is a loss of hepatic vascular bed function due to an increase in fibrotic tissue (Iwakiri, Shah, & Rockey, 2014). This phenomenon limits blood flow to the liver which inhibits lipid build up, and could likely attribute to the loss of steatosis. Furthermore, reduced hepatic vascular function directly inhibits hepatic glycogen metabolism which contributes to the observed hypoglycemia.
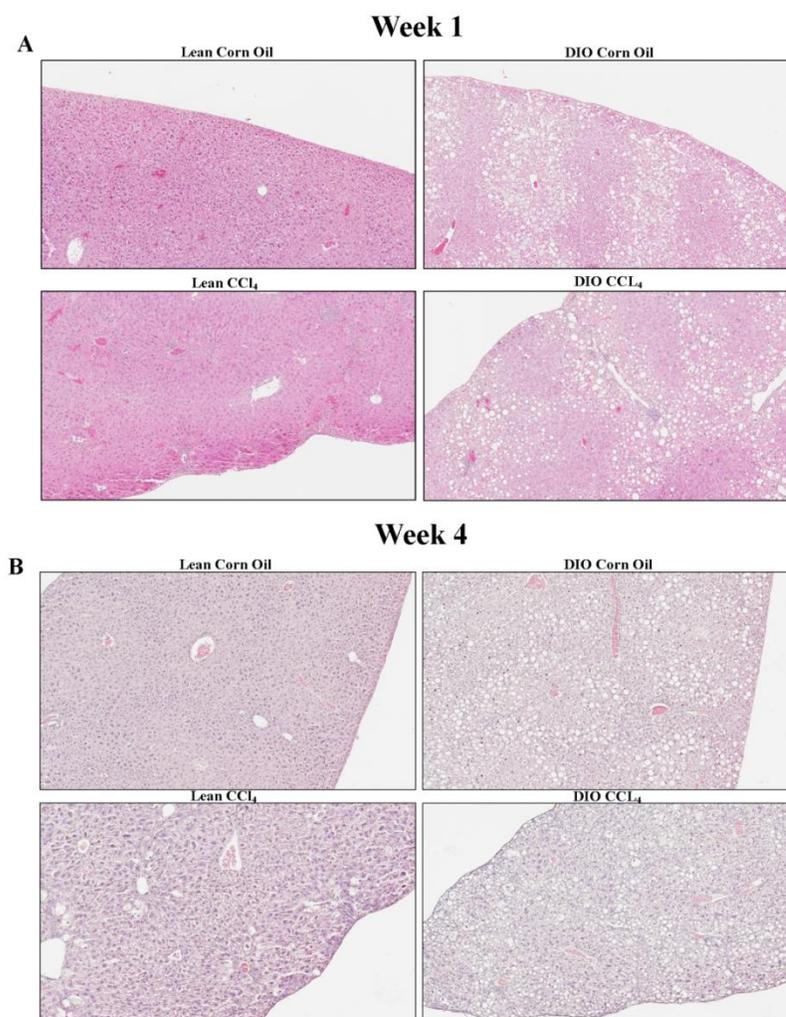
Figure 4.3. Histological evaluation of the DIO+CCL$_4$ NASH model. DIO male C57BL/6 male mice were administered CCl4 twice weekly for a period of either 1 or 4 weeks. H&E staining of two-hit model recapitulates disease pathology in liver. Representative H&E (10X) cross-sectional images captured at **(A)** week 1 and **(B)** week 4.

Hepatic secretion of fibroblast growth factor 21 (FGF21) is known to increase in obese patients and those with NALFD in response to lipotoxicity and ER stress (Dushay et al., 2010). We quantified FGF21 via ELISA from serum and isolated liver protein. After week 1, both circulating and hepatic FGF21 was higher in DIO animals and elevated in animals that had been injured with CCL$_4$ with no increase between CCl$_4$ injury alone

compared to DIO+CCl$_4$ animals. (Figure 4.4 A & C). After 4 weeks, both serum and liver

FGF21 levels in DIO animals remained elevated over lean controls. Interestingly, the

increase of FGF21 in animals following CCl$_4$ injections seen at week 1 was blunted in the

liver, and eliminated altogether in circulation of lean animals (Figure 4.4 A & B; C & D).

Similarly, there is a significant increase of FGF21 in DIO+CCl$_4$ compared to lean+CCl$_4$

injury alone (Figure 4.4 B & D). This suggests increased pathological progression of liver

disease in the two-hit model over time, and highlights the increased impact of residential

steatosis when combined with hepatic injury.
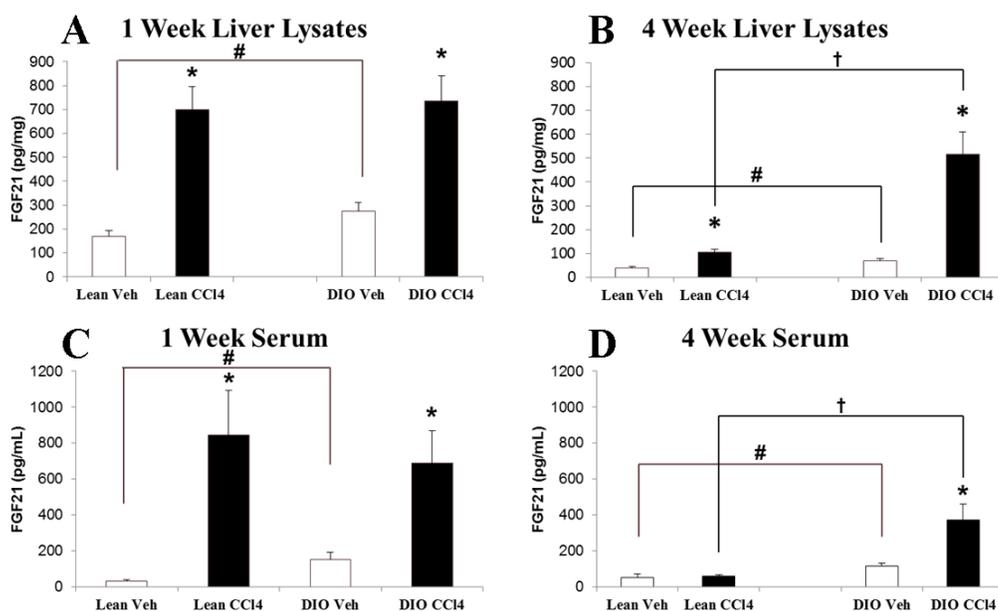
Figure 4.4 The two hit NASH model increases local and systemic levels of Fgf21.
Serum and liver Fgf21 protein was measured after 1 and 4 weeks of CCl_4 administration
in DIO mice**.** Protein expression levels of Fgf21 in liver lysates **(A & B)** and in serum **(C
& D)** were increased with CCl_4 administration at both time points. After 4 weeks,
DIO+CCl_4 animals showed increased hepatic and circulating FGF21 compared to lean
CCl_4 control animals. Data are expressed as means $\pm$ S.E.M. (n=5 mice/group).
Significance is indicated *$P \leq 0.05$, CCl4-treated group versus corn oil-treated group, # P
≤ 0.05 DIO group versus lean control group, and $\dagger$ $P \leq 0.05$ lean CCl_4-treated group
versus DIO CCl4treated group for the ELISAs and gene expression experiments
(Dunnett's one-way ANOVA).

At both the 1) early and 2) long term time points, the two-hit combination of HFD and

CCl_4 displayed ballooning hepatocytes (Figure 4.3), which are a pathological

characteristic of hepatocellular death that is visualized as markedly swollen hepatocytes

which display a pronounced cytoplasm along with nuclear hepatocellular hypertrophy.

Hepatocyte ballooning is a feature of cellular apoptosis in which ATP loss results in

intracellular calcium level increases that disrupt plasma membrane function and results in

hepatocellular swelling (Crawford, 2012). This pathology was more pronounced after 4

weeks of CCl_4 injury. Lobular inflammation in the form of increased nuclear eosin

staining near zones 2 & 3 was exhibited in the injured livers. Increased liver lobular inflammation is a result of the inflammatory response to cellular damage, tissue necrosis, and free radical presence caused by CCl_4 (Basu, 2003). Since a significant portion of the immune response is recruited to the liver from elsewhere, histological assessment shows the predominant inflammatory response near portal veins located in zone 3 (Figure 4.3). A consequence of increased hepatic inflammation in NASH is a rise in soluble CD14 protein (Ogawa et al., 2013). CD14 was quantified by ELISA and found to be increased in animals that had been injured with CCL_4, and significantly elevated in $DIO+CCl_4$ animals at both timepoints (Figure 4.5).

A related pathological feature seen in the CCl_4 challenged livers are Mallory bodies, which are present at week 1 and become more prominent after 4 weeks of CCl_4 administration (Figure 4.3) and tend to develop concurrent with the progression of fibrosis (Jeong et al., 2005). Mallory-Denk (MDB) bodies are eosinophils inclusions near nuclei of ballooning hepatocytes. The inclusions are composed of misfolded intermediate keratin filaments, ubiquitin, heat shock proteins, and p62. While the presence of MBD are not required for a NASH diagnosis, they are correlated with incidence of cirrhosis, and therefore strengthen the diagnosis (Brunt & Tiniakos, 2010).
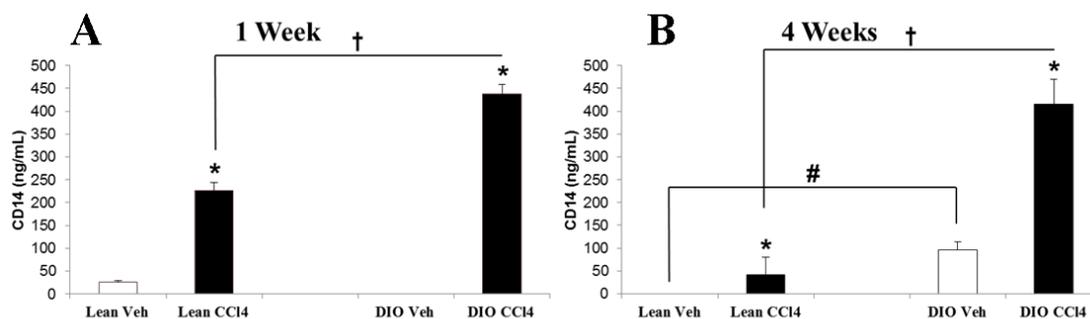
Figure 4.5 Soluble CD14 levels in circulation in NASH model. Serum levels of CD14 protein levels were measured after 1(**A**) and 4 (**B**) weeks of CCl_4 administration in DIO mice. CD14 was increased by CCl_4 treatment at 1 week independent of diet, but significantly higher in DIO+CCl_4 after 4 weeks. Data are expressed as means $\pm$ S.E.M. (n=5 mice/group). Significance is indicated *$P \leq 0.05$, CCl4-treated group versus corn oil-treated group, # $P \leq 0.05$ DIO group versus lean control group, and † $P \leq 0.05$ lean CCl_4-treated group versus DIO CCl_4treated group for the ELISAs and gene expression experiments (Dunnett's one-way ANOVA).

In order to determine collagen deposition and fibrosis, mason's trichrome staining was

performed. After one week, minor perisinusoidal fibrosis was present near zone 3,

centralized near areas with pronounced inflammation, in livers that were injured with

CCl_4. After 4 weeks of injury, the fibrosis was more pronounced, but was not

significantly impacted by the presence of steatosis in animals combined on a HFD

(Figure 4.6).

Week 1

Week 4
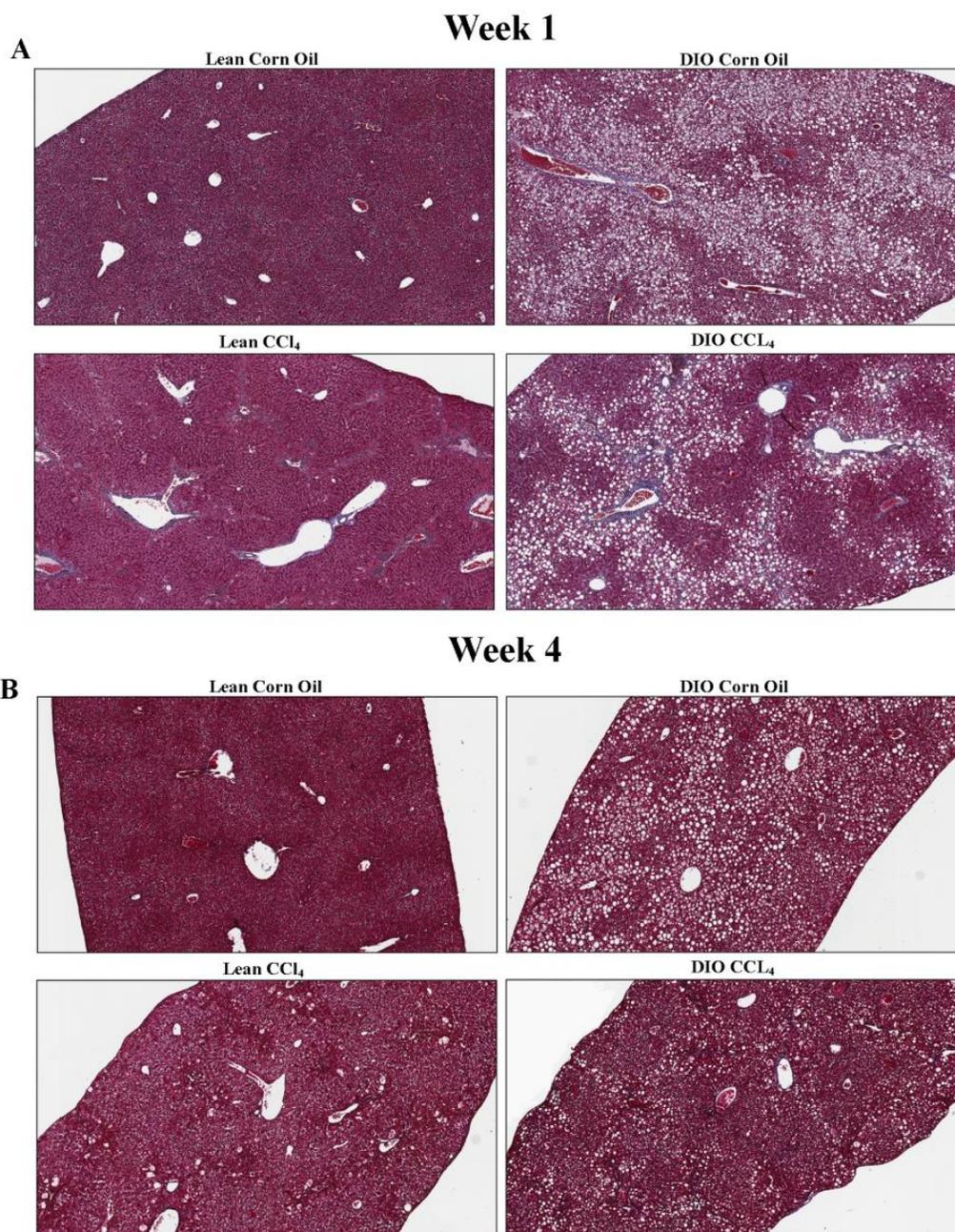
Figure 4.6 Progression of hepatic fibrosis in the two hit model of NASH. Lean and DIO male C57BL/6 mice were chronically administered CCl_4 for either 1 **(A)** or 4 **(B)** weeks. Representative cross-sectional images of trichrome stained liver sections (10X) of week 1 and week 4 displayed.

Transforming growth factor-beta (TGFβ) superfamily members and their known downstream SMAD effectors are well understood to play a role in the development of hepatic fibrosis (Xu, Liu, Zhou, & Zhang, 2016). In order to understand the response and possible role of TGFβ superfamily members in the pathology of our two-hit NASH model, we measured TGFβ, growth differentiation factor 8 (Gdf8), growth differentiation factor 15 (gdf15), inhibin-βa (inhba; subunit of Activin a), and inhibin-βb (inhbb; subunit of Activin b) RNA expression via real-time quantitative PCR (RT-qPCR) in the liver at both timepoints. When normalized to a housekeeping gene glyceraldehyde-3-phosphate dehydrogenase (gapdh), we observed a significant CCl_4 induced increase in INHBA and INHBB gene expression after 1 week independent of diet. Gdf15 was increased with CCl_4 treatment in lean mice, but not in the DIO group. This was likely a result of the basal increase in gdf15 expression caused by obesity (Figure 4.7A). At week 4, the only increased expression of Activins were in DIO+CCl_4 groups. Lean CCl_4 animals increased expression of Activin A and B had reduced to those of the control groups. Notably, DIO animals with no liver injury displayed a decrease in Activin A expression at this timepoint. Also at week 4, elevated gdf15 expression was entirely dependent on the CCl_4 injury. Curiously, Gdf8 (also known as myostatin) showed increased mRNA expression at this timepoint as well (Figure 4.7 B). This data shows the active response and possible regulatory roles TGFβ superfamly members are likely playing in our two-hit *in vivo* NASH model.
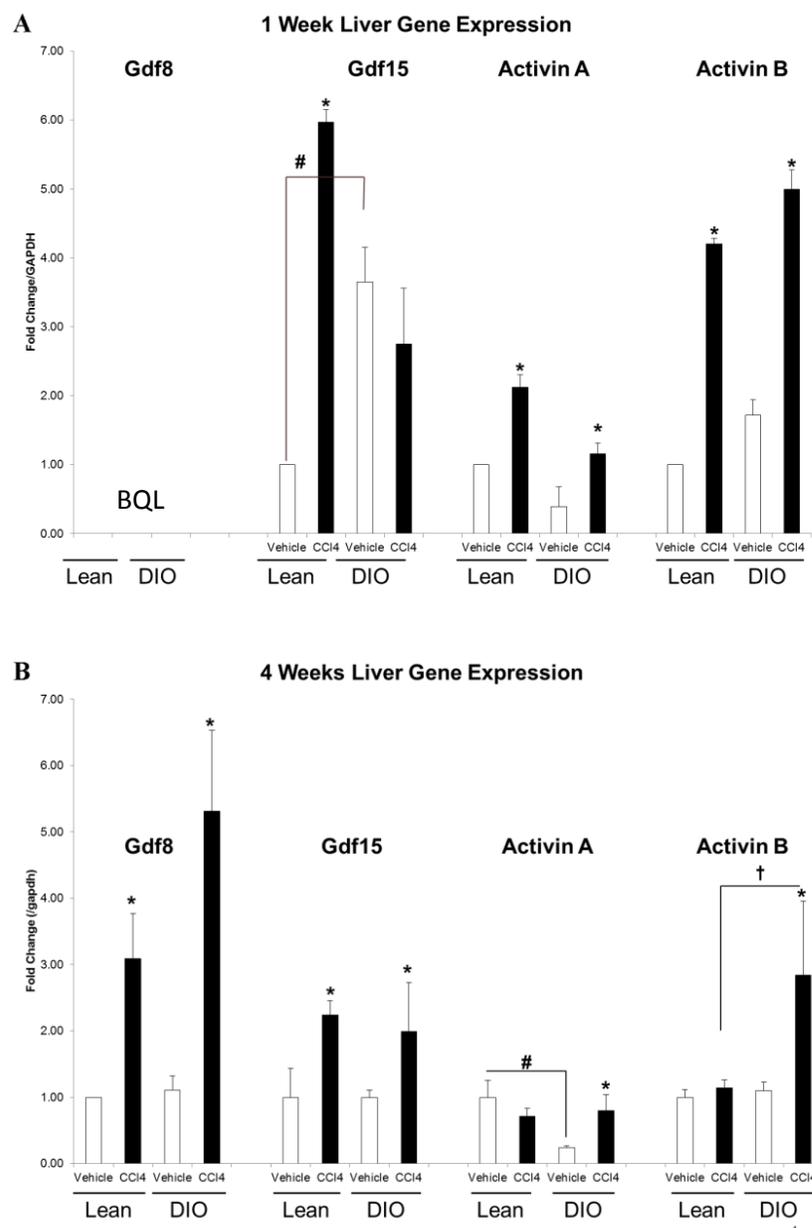
Figure 4.7. Gene expression analysis of hepatic TGFβ superfamily members. Lean and DIO male C57BL/6 mice were chronically administered CCl_4 for either 1 **(A)** or 4 **(B)** weeks. Gene expression analysis was performed by qRT-PCR on liver at 1 and 4 week post CCl_4 injury. Data are expressed as means ± S.E.M. (n=5 mice/group). Significance is indicated *P ≤ 0.05, CCl_4 treated group versus corn oil control group; † P ≤ 0.05, DIO group versus lean control group (Dunnett's one-way ANOVA).

An emerging area of interest in NASH pathology that is not well understood is the concomitant muscle atrophy observed in patients (Lee et al., 2016). In order to understand the phenomenon and possible mechanisms that drive it, we measured various markers of muscle atrophy in our two-hit model. First, we monitored weekly body composition by means of quantitative nuclear magnetic resonance (QNMR), and observed a flattening in body weight gain in the DIO+CCl$_4$ group, with no difference observed in lean animals regardless of liver injury (Figure 4.8 A). Fat-free mass (assumed to be lean mass) showed the same trend toward muscle loss in DIO+CCl$_4$ animals (Figure 4.8 B) that was confirmed by weighing gastrocnemius bundles at the time of sacrifice (Figure 4.8 C). Finally, myofiber cross-sectional area was measured in H&E stained soleus muscles that demonstrated a 41% myofiber area reduction in DIO+CCl$_4$ animals compared to the DIO control (Figure 4.8 D & E). These data clearly show a significant ability of our two-hit *in vivo* NASH model to emulate the concomitant muscle atrophy observed in NASH patients.
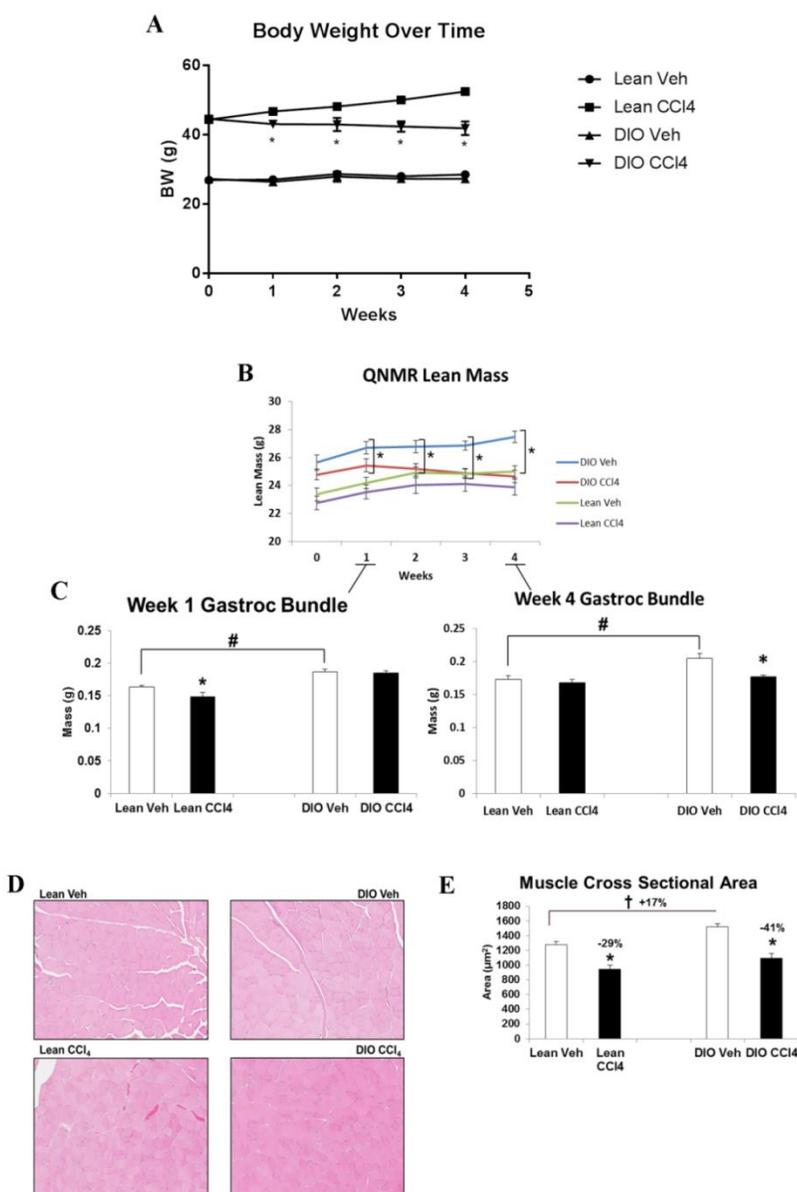
Figure 4.8 The two hit model of NASH negatively affects muscle mass. Both DIO and lean male C57BL/6 mice were chronically administered CCl$_4$ for either 1 or 4 weeks. **(A)** Body weight changes over time course in the two-hit NASH model. **(B)** QNMR body composition measurements of lean mass. **(C)** Gastrocnemius muscle mass measurements on both 1 and 4 weeks. **(D)** Representative H&E cross-sectional images of myofibers in the gastrocnemius muscle were analyzed. **(E)** Fiber diameter of gastrocnemius muscles (white-corn oil control, black-CCl$_4$). All quantifications of myofibers (~200 counted per group) were determined using ImageScope software (Aperio). Data are expressed as means ± S.E.M. (n=5 mice/group). Significance is indicated *P ≤ 0.05, CCl$_4$ treated group versus corn oil control group; † P ≤ 0.05, DIO group versus lean control group (Dunnett's one-way ANOVA).

In order to understand the mechanism of atrophy in the muscles, we analyzed mRNA expression via RT-qPCR of Gdf8, gdf15, and ubuitin ligases tripartite motif containing 63 (trim63) and F-box protein 32 (fbxo32) in gastrocnemius bundles of the animals at week 1. We observed no increases in ubuitin ligase expression or Gdf8 in DIO animals absent injury, or in lean animals who were injured with CCl_4. Gdf15 was the only injury marker that showed increased expression in DIO muscle without CCl_4 induced injury. Most notably, all 4 genes associated with muscle atrophy were significantly increased in muscles from the DIO+CCl_4 group (Figure 4.9). This data clearly demonstrates the requirement of a two-hit approach to replicate the concomitant muscle atrophy observed in NASH patients.
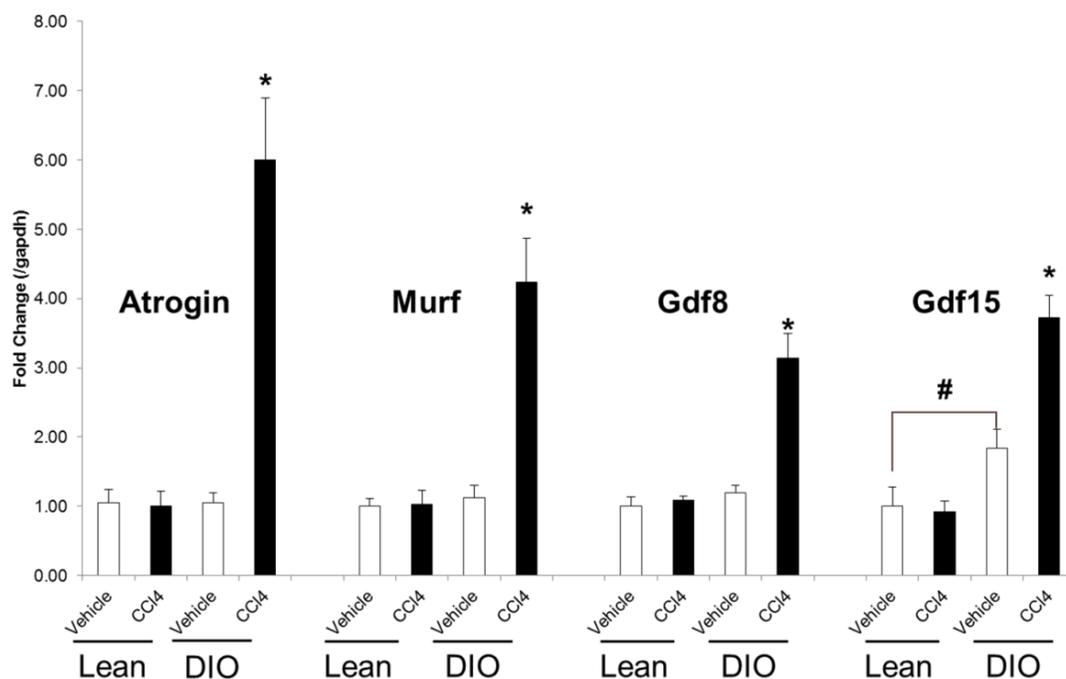
Figure 4.9 Muscle atrophy genes increased in a two-hit model of NASH. Gene exprssion analysis via qRT-PCR was performed on muscles from 1 week post CCl$_4$ injury and CCl$_4$ injury plus high fat diet (HFD). Data are expressed as means ± S.E.M. (n=5 mice/group). Significance is indicated *P ≤ 0.05, CCl$_4$ (+/- HFD) treated group versus corn oil control group (Dunnett's one-way ANOVA).

4.2   *In vitro* replication of NASH model

In order to explore the mechanisms involved in a potential liver-muscle cross tissue

endocrine relationship, we isolated liver and muscle cell types to replicate the two-hit *in*

vivo NASH model in an *in vitro* system. Our goal was to replicate the hepatic challenges

observed in the two-hit NASH model, and recreate an in vitro environment that induces

similar muscle atrophy. Primary hepatocytes were isolated from mice, and plated

overnight. The next day, the cells were challenged with a variety of chemicals in order to

replicate individual aspects of NASH pathology: CCl$_4$ to generate oxidative stress as well

as replicate the *in vivo* model, lipopolysaccharide to cause an inflammatory response, hyodrogen peroxide to generate reactive oxygen species (ROS), and thapsigargin to induce ER stress. After 1 day of exposure to various chemical challenges, hepatocyte media was collected. The media of insulted hepatocytes was diluted (1:10) and placed on mouse myoblasts cells for 5 days, which were allowed to differentiate into myotubes. Effects of muscle atrophy and reduced myoblast differentiation were monitored at the conclusion of the 5 days via image analysis of myotube diameter.

Oxidative stress by means of CCl_4

Oxidative stress is prominent player as a second hit in the development and progression of NAFLD into NASH (Basaranoglu, Basaranoglu, & Sentürk, 2013). The primary hepatotoxic mechanism of CCl_4 is the development of oxidative stress via the generation of trichloromethylperoxy free radicals (Weber et al., 2003). We induced oxidative stress in primary hepatocytes by adding CCl_4 to the media, and we saw a dose dependent increase in ALT and AST levels 24 hours later (Figure 4.10).

Figure 4.10 CCl₄ induces hepatocellular injury *in vitro*. Primary mouse hepatocytes were treated with titrated doses of CCl₄ for 24 hours. ALT **(A)** and AST **(B)** were then measured in the media. Data are expressed as means ± S.E.M. (n=3 wells/group). Significance is indicated *P ≤ 0.05, CCl₄ treated group versus vehicle control group (Dunnett's one-way ANOVA).
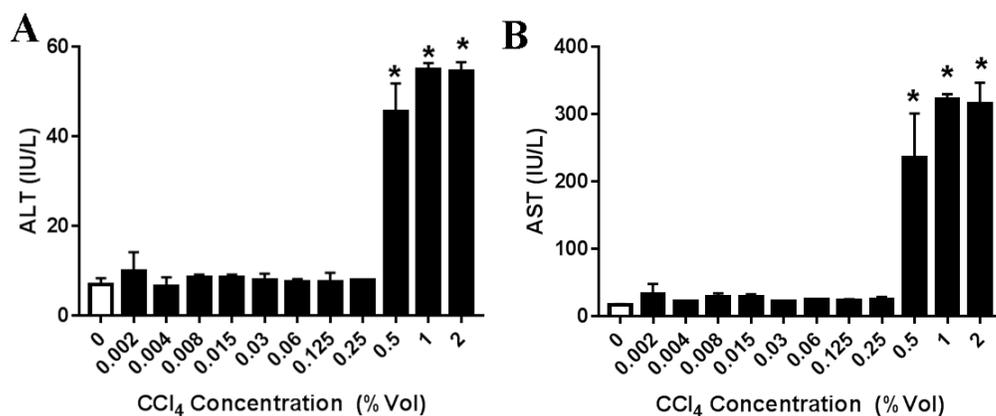
ROS generation via H_2O_2 challenge

Oxidative stress is believed to be another major contributor to the NASH sequelae.

Oxidative stress is the buildup of reactive oxygen species (ROS) (H. Fujii & Kawada,

2012) that play proinflammatory and profibrogenic roles (Chalasani, Deeg, & Crabb,

2004). In order to accurately reproduce *in vitro* oxidative stress, hepatocytes were treated

with H_2O_2. Twenty four hours after insult, ALT and AST were dose dependently

increased in the media confirming hepatocellular stress and damage (Figure 4.11).
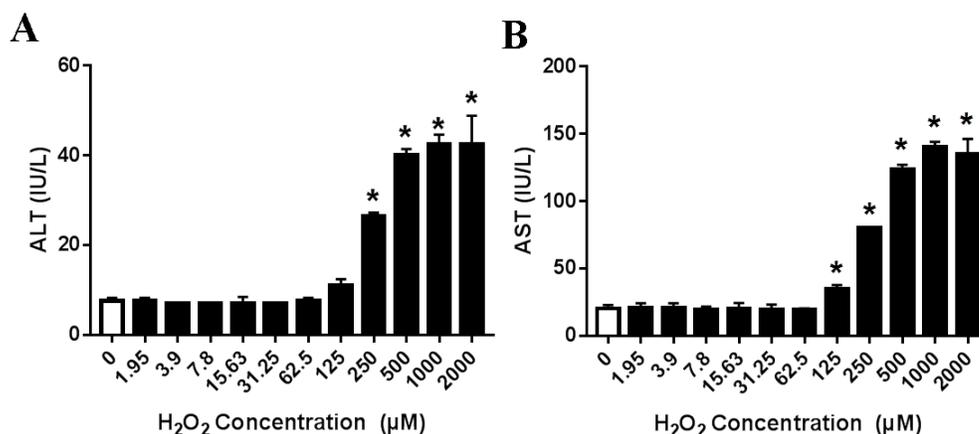
Figure 4.11 H₂O₂ induces hepatocellular injury *in vitro*. Primary mouse hepatocytes were treated with titrated doses of H_2O_2 for 24 hours. ALT **(A)** and AST **(B)** were then measured in the media. Data are expressed as means ± S.E.M. (n=3 wells/group). Significance is indicated *P ≤ 0.05, H_2O_2 treated group versus corn oil control group (Dunnett's one-way ANOVA).

Thapsigargin induced ER Stress

ER stress is a contributor to the development of NASH (Bozaykut, Sahin, Karademir, & Ozer, 2016), therefore we exposed primary hepatocytes to thapsigargin (Tg) for 24 hours (Fang et al., 2013). Thapsigargin is a selective inhibitor of the ubiquitous sarco-endoplasmic reticulum Ca^{2+}-ATPases (SERCAs). Inhibition of SERCAs blocks pumping of calcium from the cytosol into the ER lumen and results in a depletion of ER luminal calcium stores. This loss of Ca^{2+} is the primary mechanism behind the ER stress observed, and can eventually lead to induction of apoptosis (Canová, Kmoní˘ Cková, Martínek, Zídek, & Farghali, 2007). ER stress has also been linked to FGF21 secretion (Schaap, Kremer, Lamers, Jansen, & Gaemers, 2013), so we measured FGF21 protein in the hepatocyte media and saw a dose responsive increase indicative of ER stress (Figure 4.12).
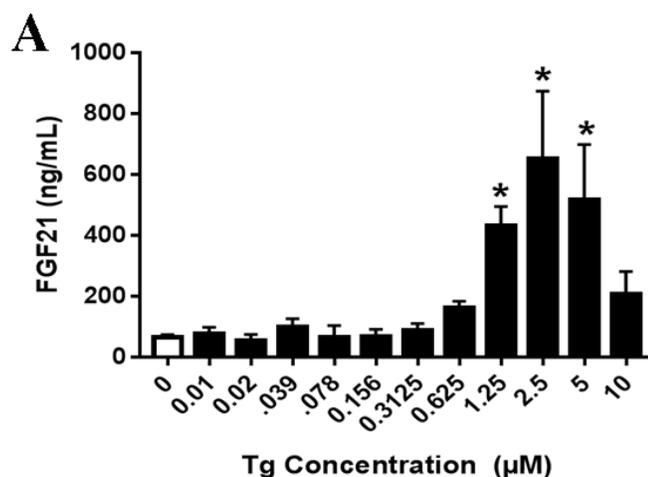
Figure 4.12 Thapsigargin induces hepatocellular ER stress *in vitro*. Primary mouse hepatocytes were treated with titrated doses of thapsigargin for 24 hours. FGF21 was then measured in the media. Data are expressed as means ± S.E.M. (n=3 wells/group). Significance is indicated *P ≤ 0.05, H_2O_2 treated group versus corn oil control group (Dunnett's one-way ANOVA).

Muscle myoblast response to hepatocellular damages

As demonstrated by our *in vivo* findings (Figure 4.8), liver injury alone or combined with diet induced obesity replicated the concomitant muscle atrophy observed in NASH patients. Next we queried if the hepatokines generated via the various modes of stress and injury would be responsible for the muscle atrophy. In doing so, we took media from our various *in vitro* insults, diluted them (1:10) and placed onto fully differentiated C2C12. Myotubes were imaged after 5 days of exposure to insulted hepatocyte media and myotube diameter and length were calculated. Treatment with the various challenges significantly reduced myotube length as determined by image analysis (Figure 4.13).
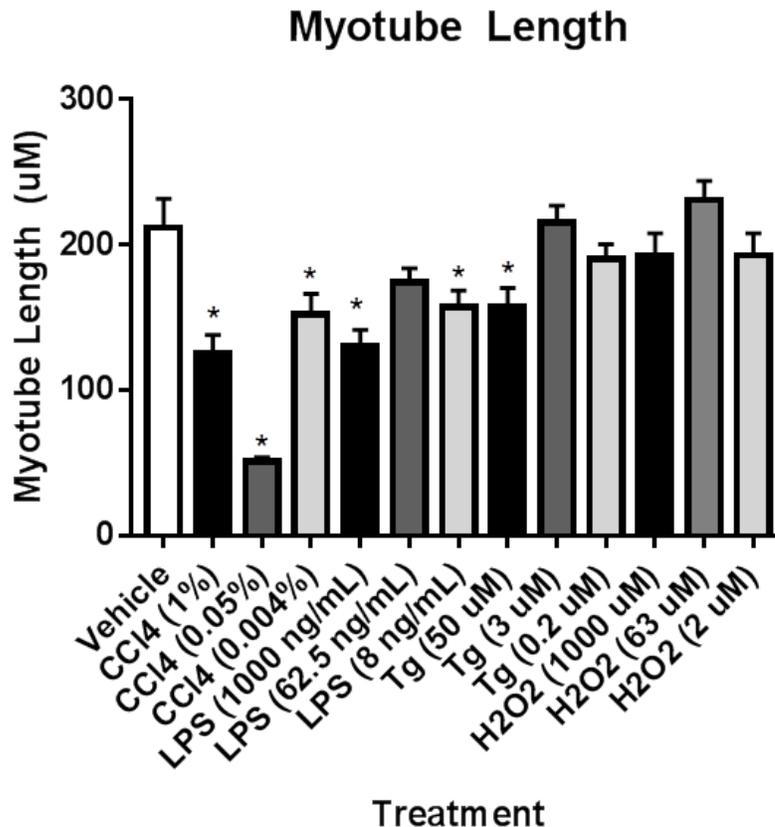
Myotube Length

Figure 4.13 Inured hepatocyte media reduces myotube diameter *in vitro*. After 5 days of daily exposure to diluted (1:10) injured hepatocyte media, myotube length was significantly reduced by CCl$_4$, LPS, and thapsigargin. Data are expressed as means ± S.E.M. (n=3 wells/group). Significance is indicated *P ≤ 0.05, treated group versus vehicle (corn oil) control group (Dunnett's one-way ANOVA).

4.3   Activin A and Gdf8 activity in NASH model

Given the increased signaling of TGFβ superfamily members and their established roles

in NAFLD and NASH (Polyzos, Kountouras, Anastasilakis, Triantafyllou, & Mantzoros,

2016), we wanted to evaluate the effects that blocking their signaling in the CCl$_4$ liver

injury model would have. Neutralization of specific TGFβ superfamily members Activin

A, Gdf8, and combination of both were compared with the effects of a pan inhibitor

soluble decoy receptor Actr2b-Fc. We wanted to simplify our first steps by performing

our experiments acutely and in lean mice to examine the effects in acute liver injury.

Antibodies were predosed 24 hours before a single administration of CCl_4 in male

C57BL/6 mice, which were sacrificed after another 24 hours. Predosing regimen was

chosen to ensure that there was proper exposure of the antibody at the onset of injury. We

analyzed biochemical assessments of liver injury: ALT, AST levels, total bilirubin, and

blood glucose. ALT and AST levels were shown to be increased in all CCl_4 treatment

groups, with no significant difference between antibody therapies (Figure 4.14).
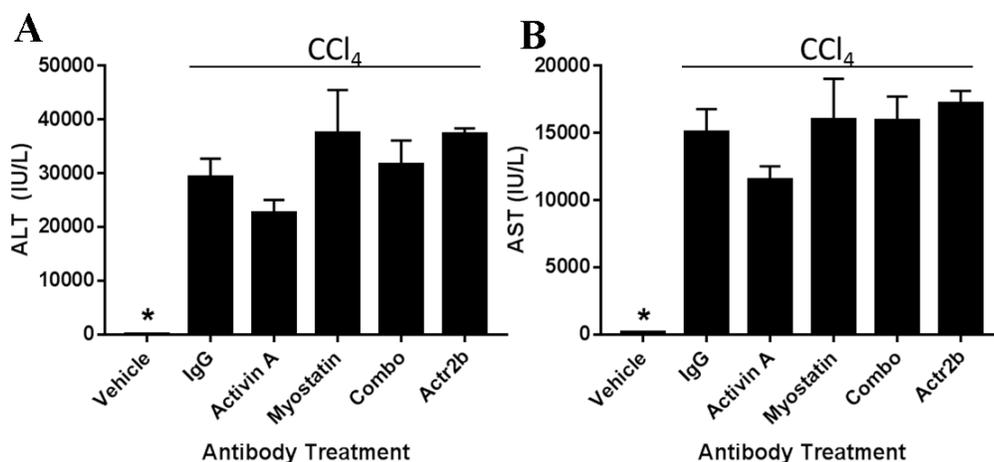
Figure 4.14 Acute effects of TGFβ family inhibition on liver injury markers. Lean
male C57BL/6 mice were pretreated with an inhibitor to the TGFβ family, followed by a
single dose of CCl_4 16 hours later. Serum levels of ALT **(A)** and AST **(B)** were measured.
Data are expressed as means ± S.E.M. (n=5 mice/group). Significance is indicated *P ≤
0.05, CCl_4 treated group versus corn oil control group (Dunnett's one-way ANOVA).

Additional liver functional markers were measured in serum (bilirubin and glucose) at the

same time point (Figure 4.15). While CCl_4 liver injury increased circulating bilirubin

levels after a single injection, Gdf8 antibody inhibition statistically improved the buildup

of these chemicals. The soluble decoy receptor Actr2b-Fc, which should also inhibit Gdf8

signaling, improved bilirubin and glucose levels as well. While circulating glucose can

come from a variety of sources, we know the acute damage to the liver in this model will

reduce hepatic gluconeogenesis (Carvalho, Jones, McGuirk, Sherry, & Malloy, 2002),

therefore we measured glucose levels as an analog of this biological function. CCl_4 injury

significantly reduced circulating glucose levels after a single dose. Interestingly,

inhibition of both Activin A and Gdf8 together slightly protected against this effect.

Furthermore, the soluble decoy receptor, which inhibits signaling of both proteins, also

improved circulating glucose levels. An insignificant trend was observed with Gdf8, but a

noteworthy finding nonetheless.
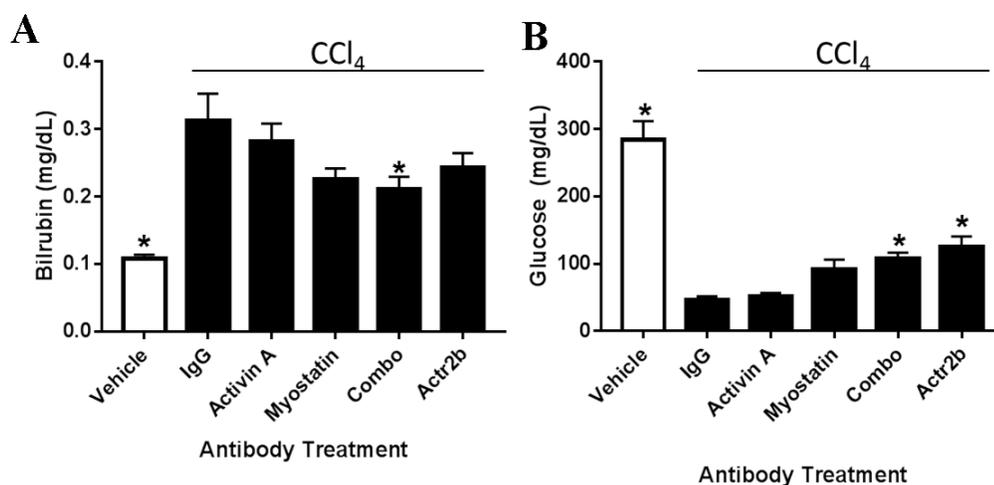
Figure 4.15 Liver function was negatively impacted by CCl_4 administration. Lean male C57BL/6 mice were pretreated with an inhibitor to the TGFβ family, followed by a single dose of CCl_4 16 hours later. Blood was then collected 24 hours after the CCl_4 dose and bilirubin **(A)** and glucose **(B)** were measured. Data are expressed as means ± S.E.M. (n=5 mice/group). Significance is indicated *P ≤ 0.05, CCl_4 treated group versus corn oil control group (Dunnett's one-way ANOVA).

Next, gene expression of several members was measured directly in liver tissue. No appreciable changes in gene expression of Inhba and Inhbb were noted (data not shown) while Gdf8 was mostly below quantifiable limits (data not shown). Intriguingly, expression of Gdf15 was attenuated with the combination antibody and ActRIIB-Fc treatment (Figure 4.16 A). Diminished expression of Gdf15 may reflect a dampened injury response to CCl_4 as it is often correlated with the magnitude of injury.

FGF21 protein levels were also measured in these samples (Figure 4.16 B). Consistent with the literature, analysis confirmed increased FGF21 protein levels acutely following CCl_4 injury. Interestingly, Gdf8 inhibition via its specific antibody increased hepatic FGF21 protein, while the pan inhibition via Actr2b-Fc did not. Furthermore, the combination of Gdf8 and Activin A neutralization had no effect on hepatic FGF21. Increased FGF21 signaling could be a mechanism by which Gdf8 inhibition is protecting the liver acutely following injury, and that effect is lost with general blocking of that signal through Activin receptor 2 B or Activin A blocking. These data suggest a novel role of hepatic Gdf8 signaling in acute CCl_4 injury that, when inhibited, appears to illicit protective effects on the liver. There is also evidence that if Activin A is neutralized in addition to Gdf8, those effects on FGF21 are lost.
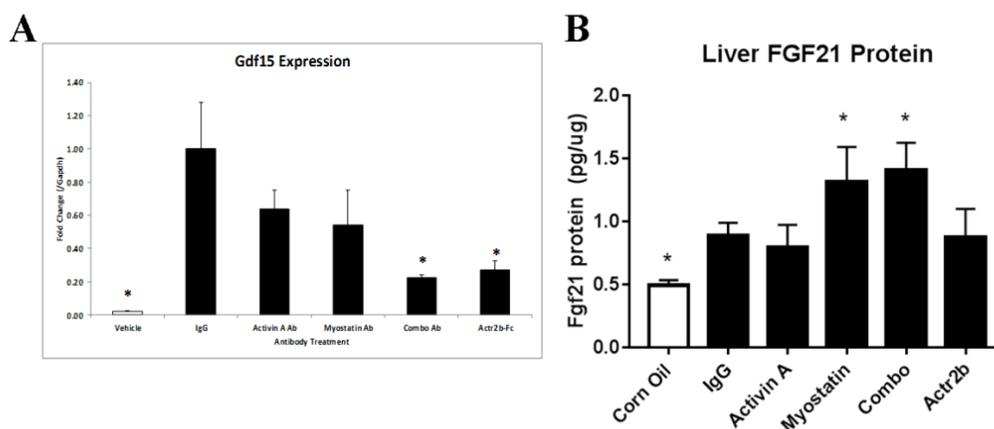
Figure 4.16 Acute injury increases secondary markers of injury. Lean male C57BL/6 mice were pretreated with an inhibitor to the TGFβ family, followed by a single dose of CCl₄ 16 hours later. Twenty four hours following the CCl₄ injection liver RNA and serum was collected. Gene expression and ELISAs performed to measure Gdf15 transcript (**A**) and Fgf21 (**B**) protein. Gdf15 gene expression was significantly reduced with combined inhibition of Gdf8 and Activin A. Liver FGF21 protein was increased by Gdf8 inhibition. Data are expressed as means ± S.E.M. (n=5 mice/group). Significance is indicated *P ≤ 0.05, CCl₄ treated group versus IgG control group (Dunnett's one-way ANOVA).

To confirm if there is any Gdf8 signaling increase in the liver at this 24 timepoint, we measured the protein expression both systemically and locally. While circulating Gdf8 was not increased at this early timepoint (data not shown), there was a considerable amount of hepatic Gdf8 protein after CCl₄ injury. Gdf8 protein was increased 24 hours after a single dose of CCl₄, and those protein levels were reduced in all antibody treated groups (Figure 4.17 A). Anti-Gdf8 antibodies (including the decoy receptor) will reduce and/or sequester Gdf8 protein. However, the reduced hepatic Gdf8 protein following anti-Activin A treatment was unexpected, and prompted us to measure circulating Activin A levels in these animals as well (Figure 4.17 B). Serum Activin A protein levels were increased with CCl₄ injury after 24 hours, and was reduced with Activin A inhibiting antibodies. Unexpectedly, inhibition of Gdf8 caused an increase in circulating Activin A

protein levels. This is a novel finding that may suggest a cross regulatory feedback,

which may have implications in hepatic injury response and disease progression.
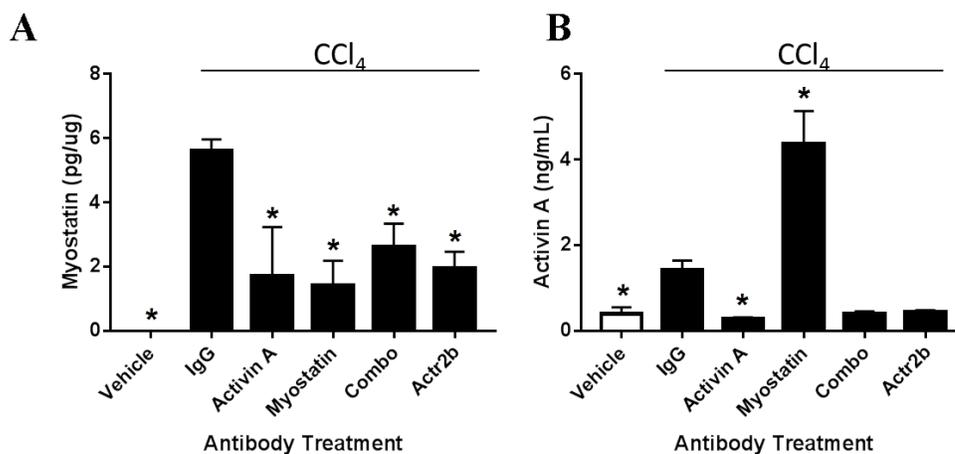
Figure 4.17 Acute liver injury increases Gdf8 and Activin A protein levels. Lean
male C57BL/6 mice were pretreated with an inhibitor to the TGFβ family, followed by a
single dose of CCl4 16 hours later. Twenty four hours following the CCl4 injection liver
serum was collected and ELISAs performed to measure Gdf8 **(A)** and Activin A **(B)**
protein. Both Activin A and Gdf8 were increased following CCl_4 injury. Inhibition of
Gdf8 increased hepatic Activin A protein beyond levels of CCl_4 injury alone. Data are
expressed as means ± S.E.M. (n=5 mice/group). Significance is indicated *$P \leq 0.05$, CCl_4
treated group versus IgG control group (Dunnett's one-way ANOVA).

In important additional ligand within the TGFβ family that shares a ligand with Activin A

and Gdf8 is Activin B. We measured serum levels of Activin B in our two hit model, and

saw increased protein expression in DIO animals, that was increased with the addition of

CCl_4 (Figure 4.18).
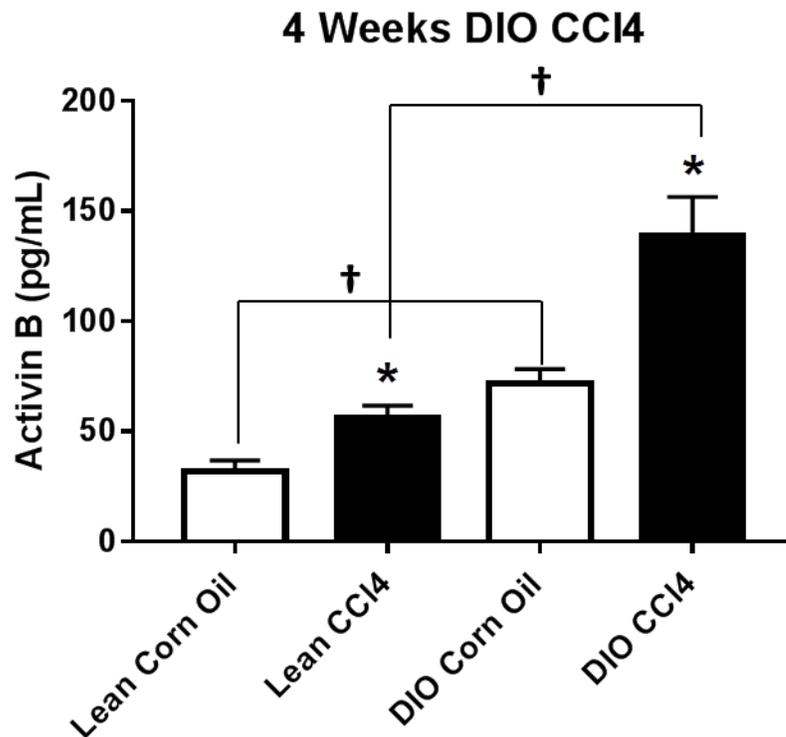
Figure 4.18 Serum Activin B increases following 4 weeks on DIO+CCl₄ NASH model. Serum levels of Activin B protein levels were measured and 4 weeks of CCl₄ administration in DIO and lean mice. Activin B was increased by CCl₄ treatment independent of diet, but significantly higher in DIO+CCl₄ after 4 weeks. Data are expressed as means ± S.E.M. (n=5 mice/group). Significance is indicated *P ≤ 0.05, CCl4-treated group versus corn oil-treated group, † P ≤ 0.05 DIO group versus lean control group receiving the same CCl₄ treatment, for the ELISA (Dunnett's one-way ANOVA).

This increase in Activin B was also observed in another model of liver fibrosis, bile duct ligation, in a timecourse study performed in rats (Figure 4.19). Together, these data display a conserved role of several TGFβ family members in response to liver injury, which could play a significant role in concimitant muscle atrophy.
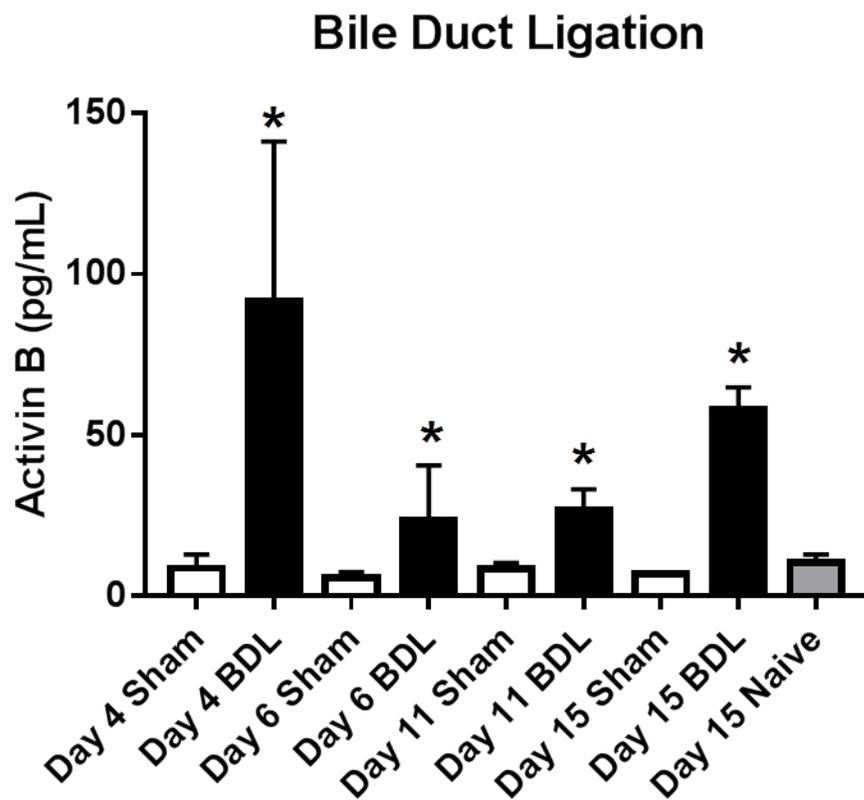
Figure 4.19 Serum Activin B protein is increased following BDL surgery. Serum levels of Activin B protein levels were measured in male Sprague dawley rats 4, 6, 11, and 15 days after bile duct ligation surgery. Data are expressed as means ± S.E.M. (n=3 rats/group). Significance is indicated *P ≤ 0.05, compared to the sham surgery at the same timepoint for the ELISA (Dunnett's one-way ANOVA).

CHAPTER 5. DISCUSSION

5.1 Characterization of two-hit *in vivo* model

A variety of animal models have been used to replicate NASH pathologies in rodents, however a majority of those models are either considerably long in duration, involve expensive genetic mutations, or lack specific aspects of the NASH disease state; most notably, fibrosis (Hebbard & George, 2011). Carbon tetrachloride (CCl_4) is a well characterized model of liver injury that quickly generates fibrosis and can eventually lead to HCC by inducing centrizonal necrosis via alteration of hepatocellular lysosomal and mitochondrial plasma membrane permeability which generates free radical buildup. This tissue damage recruits HSCs to proliferate and differentiate into myofibroblast cells that deposit ECM and collagen driven by increased TGFβ signaling which leads to development of fibrosis (T. Fujii et al., 2010). The use of a high fat diet (HFD) is common method of inducing metabolic aspects of NAFLD/NASH (primarily steatosis). The combination of the two insults has been suggested to produce pathology similar to that of NASH patients in a timely and cost-efficient manner that can elucidate mechanisms responsible for fibrosis progression (Kubota et al., 2013). A primary focus of our first study was to validate that pathologies associated with human NASH patients were presented in our *in vivo* two-hit model. Measurements of liver function (serum bilirubin and glucose) are detrimentally altered after 4 weeks of CCl_4 treatment only in animals challenged with both hits, suggestive of enhanced liver damage resulting from the resident steatosis in HFD animals. Steatosis occurs as a result of triglycerides that accumulate in the liver and generate lipotoxicity from elevated levels of free fatty acids,

cholesterol, and other lipid metabolites. As a result, inflammatory pathways, ER stress, oxidative stress, and ROS stress mechanisms are activated (Cusi, 2009). Our data supports the findings that a first hit of steatosis predisposes the animal to pathologies resulting from subsequent challenges that increased disease progression. Histological analysis of the liver from these animals displayed features characteristic of a NASH diagnosis including abundant steatosis, inflammation, hepatocellular ballooning, and fibrosis. These findings were supported by an increase in soluble CD14 and hepatocellular and circulating FGF21, which were both increased in the combination DIO+CCl$_4$ animals. Increases in soluble CD14 levels have been shown to be increased in NASH patients, and has been proposed as a biomarker for evaluation of therapeutic effects in NAFLD (Ogawa et al., 2013). Studies have demonstrated that FGF21 can ameliorate NASH pathologies, and that it plays a significant role in the progression of NAFLD (Liu, Xu, Hu, & Wang, 2015).

An unanticipated aspect of the model was an overall loss of adiposity as the study progressed, which resulted in a reduction in steatosis by week 4. DIO animals that received CCl$_4$ injuries lost approximately 6 gram loss in fat mass (data not shown) after 4 weeks. While this may ameliorate some of the peripheral metabolic complications associated with obesity, it accurately replicates conditions observed in end stage liver disease patients. Nayak *et al*. showed that of 17 NAFLD associated liver transplant patients, steatosis was "of the microvascular type and mostly inconspicuous, being minimal and mild in 5 and 4 cases respectively; moderate in 4; and marked in only one case." 5 explant samples did not exhibit steatosis at all (Nayak, Vasdev, Saigal, & Soin,

2010). Interestingly, one of the most common features observed in these patients was nodular and septal inflammation, which was present in all CCl_4 livers, and exacerbated by a HFD.

While not required for a diagnosis, several studies have shown a strong correlation between hepatic fibrosis and the severity and prognosis of NASH. Due to its multifaceted pathology, driven primarily through ROS generation, CCl_4 has been used as a model to induce liver fibrosis for decades. Our studies confirmed the presence of perisinusoidal fibrosis in animals injured with CCl_4. Unfortunately, while this model has been reported to induce severe (bridging) fibrosis in the past (T. Fujii et al., 2010), our studies did not replicate the magnitude of *in vivo* fibrosis observed in cirrhotic or severe NASH patients. Bridging fibrosis refers to ECM deposition that reaches from one portal vein to another, and its presence is a main factor when considering whether or not a patient requires a liver transplant. Due to the high regenerative capacity of rodent livers, it is difficult to generate bridging fibrosis *in vivo* without risking morbidity. Animal studies that have been able to generate this severity of fibrosis require 5-6 months of repeated insult. While this is potentially an option in lean animals, our studies that applied the combination of a HFD and repeated CCl_4 injuries leads to liver failure induced morbidity within 6 weeks. While analysis of the histology of these animals is still ongoing, a trend in severity of peripheral lean mass loss increasing morbidity of these animals was clear. Therefore, applications of this model to include metabolic syndrome are too severe to generate the most robust amounts of hepatic fibrosis. The resident conditions associated with obesity present in our two-hit model appear to enhance the morbidity of liver disease, and should

be considered a model of end stage liver failure more than NAFLD to mild NASH pathology.

The resident conditions associated with an obese state in this model (heightened inflammatory state, lipotoxicity, and hyperglycemia) were shown to increase mortality of rodents challenged with CCl_4 after 4 weeks. While these conditions were enough to be deleterious to liver injury survival outcomes, they are not entirely representative of the entire spectrum of metabolic complications present in diabetic patients. DIO animals fed a high fat chow are a accurate model of obesity that reflects many of the complications associated with T2DM, but not necessarily a Frank diabetic. DIO animals are typically mildly insulin resistant and do not display the full extent of insulin resistance or beta cell failure present in an obese diabetic individual. A potential consideration for future studies would be to include additional dietary insults (i.e. cholesterol or fructose) or utilize genetic modification (i.e. db/db or ob/ob mice) to exacerbate metabolic complications in these animals. Most importantly, after repeated administrations of CCl_4, these animals begin to lose their obese state. After the first few doses, the initial body weight loss can be partially attributed to a food intake reduction. However, as the model progresses, food intake recovers to normal rates (data not shown), but fat mass loss is still observed. This phenomenon is most likely caused by reduced hepatobiliary function resulting from inflammation and fibrosis limiting hepatic vascular flow. Importantly, body weight loss is seen in end stage liver disease patients, and can sometimes be recovered following transplant (Nishikawa & Osaki, 2015).

A contributing factor to the loss in body weight of end stage liver disease patients is a loss of muscle mass (Plank & Russell, 2015). The contributions of concomitant sarcopenia to disease pathology and survival outcomes in these patients are just now beginning to be studied, and the evidence shows a positive correlation between disease prognosis and lean mass (Carias et al., 2016). While the molecular relationship between liver disease and sarcopenia is not well understood, it is clear that the pro-regenerative capacities of both tissues (liver and muscle) share are very similar mechanisms of repair. Previous studies demonstrated that liver injury via CCl_4 reduced the capacity for muscle to regenerate following cardiotoxin induced injury, and was ameliorated by inhibiting TGFβ family members signaling through use of a pan inhibitor. Yaden *et al.*'s data suggests a similar role for TGFβ family signaling in both liver and muscle regeneration. Our data demonstrated an increase of hepatic signaling of TGFβ members Activin A and B (Chen et al., 2014) and Gdf8 (Nissinen et al., 2016) that are known to contribute to muscle atrophy. Therefore, we hypothesized that the CCl_4 dependent increase in hepatic Gdf8 and two-hit dependent increase in Activin expression contribute to concomitant muscle atrophy. The observation of a loss of lean mass was a key finding in our studies. Evidence suggests *in vivo* replication of liver disease induced sarcopenia is an important component to the pathology of the disease with a strong correlation to fibrosis severity (Koo et al., 2016).

5.2   TGFβ sgnaling in two-hit model

It has been well established that TGFβ (Sakai, Jawaid, Sasaki, Bou-Gharios, & Sakai, 2014) and Activin A (Palin et al., 2016) regulate various types of liver disease

progression. Specifically, Activin A levels have been shown to be increased in NASH

patients (Polyzos et al., 2016), while TGFβ is considered to be a potent regulator of

fibrosis in the liver and other tissues (Montano-Loza, Thandassery, & Czaja, 2016). We

confirmed increased hepatic expression of these factors in our model, but were also

interested in other members of this family. Most notably, increased hepatic expression of

the well described myokine Gdf8 is a novel finding in this model. Very little is known

about the role of Gdf8 in liver injury response. One study showed that reduced myostatin

signaling protected against diet induced hepatosteatosis (Guo, Wong, & Bhasin, 2013).

Role of another TGFβ member, Activin B, in liver disease is well characterized pro-

inflammatory agent (Canali et al., 2016). Until recently a lack of a specific detection

antibody has limited efforts to investigate its response at a protein level in various

models. Interestingly, our model shows an increase in Activin B (Figure 4.18). The

primary focus for the past few decades has been on Activin A, this regulation of Activin

B provides another integral playe rin th epathogenesis or progressin of disease. Further

studies should focus on the novel role of Activin B and its interplay with other TGFβ

superfamily proteins in hepatocellular injury repair and disease progression, as it appears

to represent an un researched potential therapeutic opportunity.

5.3   *In vitro* replication of concomitant muscle atrophy

In order to better understand the role individual pathologies associated with liver injury

have on muscle atrophy, we attempted to recreate the *in vivo* challenges of our model in

an *in vitro* setting. As the data demonstrated, aspects of ER stress and ROS generation

were sufficient to induce hepatocellular injury as measured by ALT/AST levels in the

media. In vitro hepatocellular injury was sufficient to reduce myotube diameter when placed on C2C12 muscle myoblasts. This data demonstrates that a variety of models of liver injury are capable eliciting direct negative effects on myotube health. Trendelenburg *et al*. showed that Activins and Gdf8 reduce myotube diameter and differentiation (Trendelenburg et al., 2009). Our findings demonstrated that myotube size reduction could potentially be indued by TGFβ members of hepatocyte origin, and can be ameliorated with addition of inhibiting antibodies. Followup studies are underway to evaluate hepatocelluar TGFβ family signalling following *in vitro* insult by measuring Activin, Gdf8, and TGFβ content in the media. Additionally, we intend to measure downstream Smad2/3 signaling in myotubes, which would indicate a direct role of TGFβ family signaling in myotube response to the injured hepatocyte media. An important caveat worth considering in this experiment is that the myotube media contains diluted chemical toxins used to insult the hepatocytes. This was controlled by adding CCl_4 alone into media without hepatocellular media to myotubes at equivalent concentrations (data not shown). While our AST/ALT data suggest that a 1:10 dilution shifts the concentration below the level of inducing injury, there is a risk that the presence of these chemicals is affecting the myotubes. In order to account for this, we attempted to separate the media containing hepatotoxins from those placed on the myotubes. Hepatocytes were injured with CCl_4 for 6 hours, media was removed, and fresh media lacking hepatotoxins was added. ALT/AST measurements 18 hours later showed no ALT/AST increases (data not shown). This suggests the initial 6 hour window is when hepatocellular damage takes place, or the hepatocytes are able to recover sufficiently with 18 hours removed from

insult. More work is required to determine a method for adding hepatocyte media to myotubes without also including the diluted hepatotoxin.

5.4 Inhibition of TGFβ members in two-hit model

Our studies showed that the two-hit model exhibited pathologies characteristic to NASH patients that drive concomitant muscle atrophy possibly driven by TGFβ superfamily signaling. In order to evaluate the effects of this proteins on liver and muscle pathology, we inhibited their function via antibody treatment *in vivo*. In lean animals, DIO+CCl$_4$ animals treated with combination Gdf8 and Activin A antibodies appeared to be protected from hepatic damage. Interstingly, a novel increase in circulating Activin A (more than two-fold greater than CCl$_4$ alone) was observed in animals treated with anti Gdf8 antibody along with CCl$_4$ injury. Abnormal Activin A expression is related to a variety of diseases and play an important role in acute hepatic injury response (Wang et al., 2013). Furthermore, Activin A inhibiting antibody reduced hepatic induction of Gdf8 following injury. Increased protein expression of Activin A by inhibiting Gdf8 and decresaed Gdf8 expression by inhibiting Activin A suggests a novel regulatory feedback system within the TGFβ supefamily that regulates signifcant aspects of injury response. This type of autoregulatory system within the family is not a novel finding. Activin A has been shown to regulate its inhibitor FST (Kipp et al., 2011), and conversely FST has been shown to upregulate Gdf8 expression as well (Kocamiş, Gulmez, Aslan, & Nazli, 2004). Our data suggests the discovery of a possible direct Gdf8 Activin A autoregulatory system. To this end, the source of additional Activin A will be of primary interest in future studies. Currently, RNA expression analysis of muscle and liver have shown no increases in

inhba expression (data not shown). Analysis of various potential sources (whole blood, testes, and hypothalamus) of Activin A are currently being investigated for transcriptional upregulation.

An important aspect of our *in vivo* model includes the concimitant muscle atrophy observed in NASH and end stage liver disease patients. TGFβ superfamily members Gdf8 and Activins are known to negatively effect muscle growth and regeneration. Specific inhibition of Gdf8 protected against lean mass loss, while blocking of Activin A signaling has no effect in DIO animals injured with CCl_4 for 5 weeks. Interestingly, pan inhibition of signaling via Actr2b-Fc antibody treatment significantly increased lean mass compared to animals that did not receive doses of CCl_4. This is a novel discovery of a potential additional ligand of the Activin 2b receptor that contributes to enhanced muscle pathology in liver disease. While inhibiting Activin A and Gdf8 provide protection from muscle wasting, that therapeutic approach seemingly fails to account for Activin B, which shows potential for its own role in NASH and its concomitant muscle atrophy. Potential therapies should consider this additional effector in impacting muscle health. This data strongly suggests another ligand for this receptor that is having a deleterious effect on muscle mass in our two-hit model. A proposed candidate that could be responsible for this effect is Activin B. Activin B is a ligand for the Actr2b receptor, and genetic inhibition of Activin B is known to increase muscle mass (Chen et al., 2015). Activin B protein levels were measured in our two hit model, and was shown to be increased with added challenges (Figure 4.18).

An important validation of this finding was to investigate that Activin B signaling is increased in other models of liver injury. Bile duct ligation is a surival surgery that blocks the extrahepatic biliary system which initiates a cascade of pathological outcomes resulting in cholestasis and inflammation. This injury eventually generates substantial fibrosis (Tag et al., 2015). Serum from a timecourse bile duct ligation clearly demonstrated a time dependent increase in circulating Activin B protein (Figure 4.19).

Antibodies targeted at pan inhibition of TGFβ family signaling have shown to be an effective treatment for muscle atrophy (Lach-Trifilieff et al., 2014), while Gdf8 specific antibodies have not proven to be quite as effective (Becker et al., 2015). Our studies show that Activin signaling could be a contributing factor to the increased efficacy of a pan inhibitor decoy receptor based approaches by inhibiting signaling of additional (I assume) ligands responsible for muscle atrophy. Gdf8 inhibition induced increase in Activin A protein could lead to reduced muscle health and function (Yaden et al., 2014). While increases in Activin B, which would be sequestered by a decoy receptor, observed in liver disease patients may contribute to increased skeletal muscle atrophy. Future studies to explore the regulatory feedback of Activin A and myostatin are required to evaluate the potential effects increased Activin A is having on the liver and muscles in this model. Also, hepatic and muscle effects of Activin B inhibition in models of liver disease have not yet been published. Additional analysis of this promising aspect of sarcopenia therapy are of particular interest moving forward.

5.5   Conclusions

Concomitant sarcopenia is beginning to emerge as an important pathology associated with liver disease patient outcome. Given the unmet medical need associated with NASH patients related to the growing obesity epidemic, a reliable and cost effective in vivo model is critically important. The potential impact on patient health makes it important to evaluate all underlying aspects of the disease when considering underlying mechanisms of disease progression and potential therapies. New data suggests a novel role of TGFβ family members Gdf8 and Activin B in NASH associated sarcopenia, providing potential utility for existing therapies which target pan inhibition of their receptor. In summary, these data highlight the important connection between liver disease and muscle atrophy with a specific role for the highly conserved TGFβ superfamily in these disease states.

REFERENCES

Akhurst, R. J., & Hata, A. (2012). Targeting the TGFβ signalling pathway in disease. *Nature Reviews Drug Discovery*, *11*(10), 790–811. http://doi.org/10.1038/nrd3810

Arrese, M., Cabrera, D., Kalergis, A. M., & Feldstein, A. E. (2016). Innate Immunity and Inflammation in NAFLD/NASH. *Digestive Diseases and Sciences*, *61*(5), 1294–1303. http://doi.org/10.1007/s10620-016-4049-x

Bambha, K. M., Dodge, J. L., Gralla, J., Sprague, D., & Biggins, S. W. (2015). Low, rather than high, body mass index confers increased risk for post-liver transplant death and graft loss: Risk modulated by model for end-stage liver disease. *Liver Transplantation*, *21*(10), 1286–1294. http://doi.org/10.1002/lt.24188

Basaranoglu, M., Basaranoglu, G., & Sentürk, H. (2013). From fatty liver to fibrosis: A tale of "second hit." *World Journal of Gastroenterology*, *19*(8), 1158–1165. http://doi.org/10.3748/wjg.v19.i8.1158

Basu, S. (2003). Carbon tetrachloride-induced lipid peroxidation: Eicosanoid formation and their regulation by antioxidant nutrients. *Toxicology*, *189*(1–2), 113–127. http://doi.org/10.1016/S0300-483X(03)00157-4

Bataller, R., & Brenner, D. (2005). Liver fibrosis. *The Journal of Clinical Investigation*, *115*(2), 209–218. http://doi.org/10.1172/JCI200524282.The

Becker, C., Lord, S. R., Studenski, S. A., Warden, S. J., Fielding, R. A., Recknor, C. P., … Benichou, O. (2015). Myostatin antibody (LY2495655) in older weak fallers: A proof-of-concept, randomised, phase 2 trial. *The Lancet Diabetes and Endocrinology*, *3*(12), 948–957. http://doi.org/10.1016/S2213-8587(15)00298-3

Besson-fournier, C., Latour, C., Kautz, L., Bertrand, J., Ganz, T., & Roth, M. (2012). Induction of activin B by inflammatory stimuli upregulates expression of the iron-regulatory peptide hepcidin through Smad1 / 5 / 8 signaling appeared in the paper journal (edited , typeset versions may be posted when available prior to final publication, *120*(2), 431–440. http://doi.org/10.1182/blood-2012-02-411470

Bogdanovich, S., Perkins, K. J., Krag, T. O. B., Whittemore, L.-A., & Khurana, T. S. (2005). Myostatin propeptide-mediated amelioration of dystrophic pathophysiology. *The FASEB Journal : Official Publication of the Federation of American Societies for Experimental Biology*, *19*(6), 543–549. http://doi.org/10.1096/fj.04-2796com

Bozaykut, P., Sahin, A., Karademir, B., & Ozer, N. K. (2016). Endoplasmic Reticulum Stress Related Molecular Mechanisms in Nonalcoholic Steatohepatitis. *Mechanisms of Ageing and Development*, *157*, 17–29. http://doi.org/10.1016/j.mad.2016.07.001

Brown, M. L., & Schneyer, A. L. (2010). Emerging roles for the TGFβ family in pancreatic β-cell homeostasis. *Trends in Endocrinology & Metabolism*, *21*(7), 441–448. http://doi.org/10.1016/j.tem.2010.02.008

Brunt, E. M., & Tiniakos, D. G. (2010). Histopathology of nonalcoholic fatty liver disease. *World Journal of Gastroenterology*, *16*(42), 5286–5296. http://doi.org/10.3748/wjg.v16.i42.5286

Buzzetti, E., Pinzani, M., & Tsochatzis, E. A. (2016). The multiple-hit pathogenesis of non-alcoholic fatty liver disease (NAFLD). *Metabolism*, *65*(8), 1–11. http://doi.org/10.1016/j.metabol.2015.12.012

Camporez, J. G., Petersen, M. C., Abudukadier, A., Moreira, G. V, Jurczak, M. J., Friedman, G., … Shulman, G. I. (2016). Anti-myostatin antibody increases muscle mass and strength and improves insulin sensitivity in old mice. *Proceedings of the National Academy of Sciences of the United States of America*, *113*(8), 2212–7. http://doi.org/10.1073/pnas.1525795113

Canali, S., Core, A. B., Zumbrennen-Bullough, K. B., Merkulova, M., Wang, C. Y., Schneyer, A. L., … Babitt, J. L. (2016). Activin B induces noncanonical SMAD1/5/8 signaling via BMP type I receptors in hepatocytes: Evidence for a role in hepcidin induction by inflammation in male mice. *Endocrinology*, *157*(3), 1146–1162. http://doi.org/10.1210/en.2015-1747

Canová, N. K., Kmoní˘ Cková, E., Martínek, J., Zídek, Z., & Farghali, H. (2007). Thapsigargin, a selective inhibitor of sarco-endoplasmic reticulum Ca 2+ -ATPases, modulates nitric oxide production and cell death of primary rat hepatocytes in culture. *Cell Biol Toxicol*, *23*, 337–354. http://doi.org/10.1007/s10565-007-0185-6

Carias, S., Castellanos, A. L., Vilchez, V., Nair, R., Dela Cruz, A. C., Watkins, J., … Gedaly, R. (2016). Nonalcoholic steatohepatitis is strongly associated with sarcopenic obesity in patients with cirrhosis undergoing liver transplant evaluation. *Journal of Gastroenterology and Hepatology*, *31*(3), 628–633. http://doi.org/10.1111/jgh.13166

Carney, E. M., Banerjee, P., Ellis, C. L., Albadine, R., Sharma, R., Chaux, A. M., … Netto, G. J. (2011). PAX2(−)/PAX8(−)/Inhibin A(+) Immunoprofile in Hemangioblastoma. *The American Journal of Surgical Pathology*, *35*(2), 262–267. http://doi.org/10.1097/PAS.0b013e3182064d11

Carvalho, R. A., Jones, J. G., McGuirk, C., Sherry, A. D., & Malloy, C. R. (2002). Hepatic gluconeogenesis and Krebs cycle fluxes in a CCL4 model of acute liver failure. *NMR in Biomedicine*, *15*(1), 45–51. http://doi.org/10.1002/nbm.745

Chalasani, N., Deeg, M. A., & Crabb, D. W. (2004). Systemic levels of lipid peroxidation and its metabolic and dietary correlates in patients with nonalcoholic steatohepatitis. *American Journal of Gastroenterology*, *99*(8), 1497–1502. http://doi.org/10.1111/j.1572-0241.2004.30159.x

Chen, J. L., Walton, K. L., Winbanks, C. E., Murphy, K. T., Thomson, R. E., Makanji, Y., … Gregorevic, P. (2014). Elevated expression of activins promotes muscle wasting and cachexia. *FASEB Journal*, *28*(4), 1711–1723. http://doi.org/10.1096/fj.13-245894

Chen, J. L., Walton, K. L., Al-Musawi, S. L., Kelly, E. K., Qian, H., La, M., … Harrison, C. A. (2015). Development of Novel Activin-Targeted Therapeutics. *Molecular Therapy*, *23*(3), 434–444. http://doi.org/10.1038/mt.2014.221

Chen, W., Woodruff, T. K., & Mayo, K. E. (2000). Activin A-induced HepG2 liver cell apoptosis: Involvement of activin receptors and Smad proteins. *Endocrinology*, *141*(3), 1263–1272. http://doi.org/10.1210/en.141.3.1263

Coleman, S. K., Rebalka, I. A., D'Souza, D. M., Deodhare, N., Desjardins, E. M., & Hawke, T. J. (2016). Myostatin inhibition therapy for insulin-deficient type 1 diabetes. *Scientific Reports*, *6*(August), 32495. http://doi.org/10.1038/srep32495

Crawford, J. M. (2012). Histologic Findings in Alcoholic Liver Disease. *Clinics in Liver Disease*, *16*(4), 699–716. http://doi.org/10.1016/j.cld.2012.08.004

Cusi, K. (2012). Role of obesity and lipotoxicity in the development of nonalcoholic steatohepatitis: Pathophysiology and clinical implications. *Gastroenterology*, *142*(4), 711–725.e6. http://doi.org/10.1053/j.gastro.2012.02.003

Cusi, K. (2009). Role of Insulin Resistance and Lipotoxicity in Non-Alcoholic Steatohepatitis. *Clinics in Liver Disease*, *13*(4), 545–563. http://doi.org/10.1016/j.cld.2009.07.009

Dasarathy, S. (2016). Cause and management of muscle wasting in chronic liver disease. *Current Opinion in Gastroenterology*, 159–165. http://doi.org/10.1097/MOG.0000000000000261

Ding, Z.-Y., Jin, G.-N., Wang, W., Sun, Y.-M., Chen, W.-X., Chen, L., … Chen, X.-P. (2016). Activin A-Smad Signaling Mediates Connective Tissue Growth Factor Synthesis in Liver Progenitor Cells. *International Journal of Molecular Sciences*, *17*(3), 408. http://doi.org/10.3390/ijms17030408

Dooley, S., & Ten Dijke, P. (2012). TGF-?? in progression of liver disease. *Cell and Tissue Research*, *347*(1), 245–256. http://doi.org/10.1007/s00441-011-1246-y

Dowman, J. K., Tomlinson, J. W., & Newsome, P. N. (2011). Systematic review: the diagnosis and staging of non-alcoholic fatty liver disease and non-alcoholic steatohepatitis. *Alimentary Pharmacology & Therapeutics*, *33*(5), 525–40. http://doi.org/10.1111/j.1365-2036.2010.04556.x

Dushay, J., Chui, P. C., Gopalakrishnan, G. S., Varela-Rey, M., Crawley, M., Fisher, F. M., … Maratos-Flier, E. (2010). Increased fibroblast growth factor 21 in obesity and nonalcoholic fatty liver disease. *Gastroenterology*, *139*(2), 456–463. http://doi.org/10.1053/j.gastro.2010.04.054

Elkina, Y., von Haehling, S., Anker, S. D., & Springer, J. (2011). The role of myostatin in muscle wasting: An overview. *Journal of Cachexia, Sarcopenia and Muscle*. http://doi.org/10.1007/s13539-011-0035-5

Endo, D., Kogure, K., Hasegawa, Y., Maku-uchi, M., & Kojima, I. (2004). Activin A augments vascular endothelial growth factor activity in promoting branching tubulogenesis in hepatic sinusoidal endothelial cells. *Journal of Hepatology*, *40*(3), 399–404. http://doi.org/10.1016/j.jhep.2003.11.019

Fajardo, R. J., Manoharan, R. K., Pearsall, R. S., Davies, M. V., Marvell, T., Monnell, T. E., … Bouxsein, M. L. (2010). Treatment with a soluble receptor for activin improves bone mass and structure in the axial and appendicular skeleton of female cynomolgus macaques (Macaca fascicularis). *Bone*, *46*(1), 64–71. http://doi.org/10.1016/j.bone.2009.09.018

Fang, D. L., Wan, Y., Shen, W., Cao, J., Sun, Z. X., Yu, H. H., … Ning, B. (2013). Endoplasmic reticulum stress leads to lipid accumulation through upregulation of SREBP-1c in normal hepatic and hepatoma cells. *Molecular and Cellular Biochemistry*, *381*(1–2), 127–137. http://doi.org/10.1007/s11010-013-1694-7

Fausto, N., Campbell, J. S., & Riehle, K. J. (2006). Liver regeneration. *Hepatology (Baltimore, Md.)*, *43*(2 Suppl 1), S45–S53. http://doi.org/10.1002/hep.20969

Font-Burgada, J., Shalapour, S., Ramaswamy, S., Hsueh, B., Rossell, D., Umemura, A., … Karin, M. (2015). Hybrid Periportal Hepatocytes Regenerate the Injured Liver without Giving Rise to Cancer. *Cell*, *162*(4), 766–779. http://doi.org/10.1016/j.cell.2015.07.026

Fougère-Deschatrette, C., Imaizumi-Scherrer, T., Strick-Marchand, H., Morosan, S., Charneau, P., Kremsdorf, D., … Weiss, M. C. (2006). Plasticity of hepatic cell differentiation: bipotential adult mouse liver clonal cell lines competent to differentiate in vitro and in vivo. *Stem Cells (Dayton, Ohio)*, *24*(9), 2098–109. http://doi.org/10.1634/stemcells.2006-0009

Fujii, H., & Kawada, N. (2012). Inflammation and fibrogenesis in steatohepatitis. *Journal of Gastroenterology*, *47*(3), 215–225. http://doi.org/10.1007/s00535-012-0527-x

Fujii, T., Fuchs, B. C., Yamada, S., Lauwers, G. Y., Kulu, Y., Goodwin, J. M., … Tanabe, K. K. (2010). Mouse model of carbon tetrachloride induced liver fibrosis: Histopathological changes and expression of CD133 and epidermal growth factor. *BMC Gastroenterology*, *10*, 79. http://doi.org/10.1186/1471-230X-10-79

Garg, Abhimanyu and Misra, A. (2002). Editorial : Hepatic Steatosis , Insulin Resistance , and. *The Journal of Clinical Endocrinology & Metabolism*, *87*(September), 3019–3022.

Gilson, H., Schakman, O., Kalista, S., Lause, P., Tsuchida, K., & Thissen, J.-P. (2009). Follistatin induces muscle hypertrophy through satellite cell proliferation and inhibition of both myostatin and activin. *American Journal of Physiology. Endocrinology and Metabolism*, *297*(1), E157–E164. http://doi.org/10.1152/ajpendo.00193.2009

Gold, E. J., Zhang, X., Wheatley, a. M., Mellor, S. L., Cranfield, M., Risbridger, G. P., … Fleming, J. S. (2005). betaA- and betaC-activin, follistatin, activin receptor mRNA and betaC-activin peptide expression during rat liver regeneration. *Journal of Molecular Endocrinology*, *34*, 505–515. http://doi.org/10.1677/jme.1.01657

Guo, W., Wong, S., & Bhasin, S. (2013). AAV-Mediated Administration of Myostatin Pro-Peptide Mutant in Adult Ldlr Null Mice Reduces Diet-Induced Hepatosteatosis and Arteriosclerosis. *PLoS ONE*, *8*(8). http://doi.org/10.1371/journal.pone.0071017

Hamrick, M. W., Arounleut, P., Kellum, E., Cain, M., Immel, D., & Liang, L.-F. (2010). Recombinant myostatin (GDF-8) propeptide enhances the repair and regeneration of both muscle and bone in a model of deep penetrant musculoskeletal injury. *The Journal of Trauma*, *69*(3), 579–83. http://doi.org/10.1097/TA.0b013e3181c451f4

He, L., Vichev, K., Macharia, R., Huang, R., Christ, B., Patel, K., & Amthor, H. (2005). Activin A inhibits formation of skeletal muscle during chick development. *Anatomy and Embryology*, *209*(5), 401–407. http://doi.org/10.1007/s00429-005-0454-1

Hebbard, L., & George, J. (2011). Animal models of nonalcoholic fatty liver disease. *World Journal of Gastroenterology*, *8*(1), 35–44. http://doi.org/10.3748/wjg.v18.i19.2300

Horiguchi, N., Lafdil, F., Miller, A. M., Park, O., Wang, H., Rajesh, M., … Gao, B. (2010). Dissociation between liver inflammation and hepatocellular damage induced by carbon tetrachloride in myeloid cell-specific signal transducer and activator of transcription 3 gene knockout mice. *Hepatology (Baltimore, Md.)*, *51*(5), 1724–34. http://doi.org/10.1002/hep.23532

Huet, C., Li, Z. F., Liu, H. Z., Black, R. A., Galliano, M. F., Engvall, E., … McNally, E. (2001). Skeletal muscle cell hypertrophy induced by inhibitors of metalloproteases; myostatin as a potential mediator. *American Journal of Physiology. Cell Physiology*, *281*(5), C1624-34. http://doi.org/10.1016/s0014-5793(00)01528-3

Hully, J. R., Chang, L., Schwall, R. H., Widmer, H. R., Terrell, T. G., & Gillett, N. A. (1994). Induction of apoptosis in the murine liver with recombinant human activin A. *Hepatology*. http://doi.org/S0270913994003101 [pii]

Iwakiri, Y., Shah, V., & Rockey, D. C. (2014). Vascular pathobiology in chronic liver disease and cirrhosis - Current status and future directions. *Journal of Hepatology*, *61*(4), 912–924. http://doi.org/10.1016/j.jhep.2014.05.047

Jeong, W., Jeong, D., Do, S., Yang, H., Hong, I., Chang, S., … Jeong, K. (2005). Expression of Cytokeratins 8 and 18 on Mallory Body and Oval Cell in Rats during Hepatic Fibrosis. *International Journal of Experimental and Clinical Pathophysiology and Drug Research*, *776*, 769–775.

Kawabata, M., Imamura, T., & Miyazono, K. (1998). Signal transduction by bone morphogenetic proteins. *Cytokine & Growth Factor Reviews*, *9*(1), 49–61. http://doi.org/10.1016/S1359-6101(97)00036-1

Kipp, J. L., Golebiowski, A., Rodriguez, G., Demczuk, M., Kilen, S. M., & Mayo, K. E. (2011). Gene expression profiling reveals Cyp26b1 to be an activin regulated gene involved in ovarian granulosa cell proliferation. *Endocrinology*, *152*(1), 303–312. http://doi.org/10.1210/en.2010-0749

Kneeman, J. M., Misdraji, J., & Corey, K. E. (2012). Secondary causes of nonalcoholic fatty liver disease. *Therapeutic Advances in Gastroenterology*, *5*(3), 199–207. http://doi.org/10.1177/1756283X11430859

Kocamiş, H., Gulmez, N., Aslan, S., & Nazli, M. (2004). Follistatin alters myostatin gene expression in C2C12 muscle cells. *Acta Veterinaria Hungarica*, *52*(2), 135–141. http://doi.org/10.1556/AVet.52.2004.2.1

Kogure, K., Omata, W., Kanzaki, M., Zhang, Y. Q., Yasuda, H., Mine, T., & Kojima, I. (1995). A single intraportal administration of follistatin accelerates liver regeneration in partially hepatectomized rats. *Gastroenterology*, *108*(4), 1136–1142. http://doi.org/10.1016/0016-5085(95)90212-0

Koo, B. K., Kim, D., Joo, S. K., Kim, J. H., Chang, M. S., Kim, B. G., … Kim, W. (2016). Sarcopenia is an independent risk factor for non-alcoholic steatohepatitis and significant fibrosis. *Journal of Hepatology*, *xxx*, 1–9. http://doi.org/10.1016/j.jhep.2016.08.019

Kruszynska, Y., Williams, N., Perry, M., & Home, P. (1988). The relationship between insulin sensitivity and skeletal muscle enzyme activities in hepatic cirrhosis. *Hepatology*, *8*(6), 1615–1619. http://doi.org/S0270913988001740 [pii]

Kubota, N., Kado, S., Kano, M., Masuoka, N., Nagata, Y., Kobayashi, T., … Ishikawa, F. (2013). A high-fat diet and multiple administration of carbon tetrachloride induces liver injury and pathological features associated with non-alcoholic steatohepatitis in mice. *Clinical and Experimental Pharmacology and Physiology*, *40*(7), 422–430. http://doi.org/10.1111/1440-1681.12102

Lach-Trifilieff, E., Minetti, G. C., Sheppard, K., Ibebunjo, C., Feige, J. N., Hartmann, S., … Glass, D. J. (2014). An Antibody Blocking Activin Type II Receptors Induces Strong Skeletal Muscle Hypertrophy and Protects from Atrophy. *Molecular and Cellular Biology*, *34*(4), 606–618. http://doi.org/10.1128/MCB.01307-13

Lagna, G., Hata, a, Hemmati-Brivanlou, a, & Massagué, J. (1996). Partnership between DPC4 and SMAD proteins in TGF-beta signalling pathways. *Nature*. http://doi.org/10.1038/383832a0

Lee, S.-J. (2007). Quadrupling muscle mass in mice by targeting TGF-beta signaling pathways. *PloS One*, *2*(8), e789. http://doi.org/10.1371/journal.pone.0000789

Lee, S.-J., Reed, L. a, Davies, M. V, Girgenrath, S., Goad, M. E. P., Tomkinson, K. N., … Wolfman, N. M. (2005). Regulation of muscle growth by multiple ligands signaling through activin type II receptors. *Proceedings of the National Academy of Sciences of the United States of America*, *102*(50), 18117–18122. http://doi.org/10.1073/pnas.0505996102

Lee, Y. ho, Kim, S. U., Song, K., Park, J. Y., Kim, D. Y., Ahn, S. H., … Han, K. H. (2016). Sarcopenia is associated with significant liver fibrosis independently of obesity and insulin resistance in nonalcoholic fatty liver disease: Nationwide surveys (KNHANES 2008-2011). *Hepatology*, *63*(3), 776–786. http://doi.org/10.1002/hep.28376

Leto, G. (2010). Activin a and bone metastasis. *Journal of Cellular Physiology*. http://doi.org/10.1002/jcp.22272

Leto, G., Incorvaia, L., Badalamenti, G., Tumminello, F. M., Gebbia, N., Flandina, C., … Rini, G. (2006). Activin A circulating levels in patients with bone metastasis from breast or prostate cancer. *Clinical & Experimental Metastasis*, *23*(2), 117–122. http://doi.org/10.1007/s10585-006-9010-5

Liu, J., Xu, Y., Hu, Y., & Wang, G. (2015). The role of fibroblast growth factor 21 in the pathogenesis of non-alcoholic fatty liver disease and implications for therapy. *Metabolism: Clinical and Experimental*, *64*(3), 380–390. http://doi.org/10.1016/j.metabol.2014.11.009

Lotinun, S., Pearsall, R. S., Davies, M. V., Marvell, T. H., Monnell, T. E., Ucran, J., … Baron, R. (2010). A soluble activin receptor Type IIA fusion protein (ACE-011) increases bone mass via a dual anabolic-antiresorptive effect in Cynomolgus monkeys. *Bone*, *46*(4), 1082–1088. http://doi.org/10.1016/j.bone.2010.01.370

MacHado, M. V., & Diehl, A. M. (2016). Pathogenesis of Nonalcoholic Steatohepatitis. *Gastroenterology*, *150*(8), 1769–1777. http://doi.org/10.1053/j.gastro.2016.02.066

McCroskery, S., Thomas, M., Maxwell, L., Sharma, M., & Kambadur, R. (2003). Myostatin negatively regulates satellite cell activation and self-renewal. *Journal of Cell Biology*, *162*(6), 1135–1147. http://doi.org/10.1083/jcb.200207056

McFarlane, C., Hennebry, A., Thomas, M., Plummer, E., Ling, N., Sharma, M., & Kambadur, R. (2008). Myostatin signals through Pax7 to regulate satellite cell self-renewal. *Experimental Cell Research*, *314*(2), 317–329. http://doi.org/10.1016/j.yexcr.2007.09.012

Mellor, S. L., Ball, E. M. a, O'Connor, A. E., Ethier, J.-F., Cranfield, M., Schmitt, J. F., … Risbridger, G. P. (2003). Activin betaC-subunit heterodimers provide a new mechanism of regulating activin levels in the prostate. *Endocrinology*. http://doi.org/10.1210/en.2003-0225\ren.2003-0225 [pii]

Mellor, S. L., Cranfield, M., Ries, R., Pedersen, J., Cancilla, B., Kretser, D. D. E., … K, D. (2000). Human Prostate and Evidence for Formation of New Activin Heterodimers of $_{NL}$ C -Subunit *, *85*(12).

Menthena, A., Koehler, C. I., Sandhu, J. S., Yovchev, M. I., Hurston, E., Shafritz, D. A., & Oertel, M. (2011). Activin A, p15INK4b signaling, and cell competition promote stem/progenitor cell repopulation of livers in aging rats. *Gastroenterology*, *140*(3), 1009–1020. http://doi.org/10.1053/j.gastro.2010.12.003

Michalopoulos, G. K. (2007). Liver regeneration. *Journal of Cellular Physiology*. http://doi.org/10.1002/jcp.21172

Montano-Loza, A. J. (2014). Skeletal muscle abnormalities and outcomes after liver transplantation. *Liver Transplantation*, *20*(11), 1293–1295. http://doi.org/10.1002/lt.23995

Montano-Loza, A. J., Thandassery, R. B., & Czaja, A. J. (2016). Targeting Hepatic Fibrosis in Autoimmune Hepatitis. *Digestive Diseases and Sciences*, *61*(11), 1–22. http://doi.org/10.1007/s10620-016-4254-7

Murphy, K. T., Cobani, V., Ryall, J. G., Ibebunjo, C., & Lynch, G. S. (2011). Acute antibody-directed myostatin inhibition attenuates disuse muscle atrophy and weakness in mice. *Journal of Applied Physiology (Bethesda, Md. : 1985)*, *110*(4), 1065–72. http://doi.org/10.1152/japplphysiol.01183.2010

Nayak, N. C., Vasdev, N., Saigal, S., & Soin, A. S. (2010). End-stage nonalcoholic fatty liver disease: evaluation of pathomorphologic features and relationship to cryptogenic cirrhosis from study of explant livers in a living donor liver transplant program. *Human Pathology*, *41*(3), 425–430. http://doi.org/10.1016/j.humpath.2009.06.021

Neuschwander-Tetri, B. A. (2010). Hepatic lipotoxicity and the pathogenesis of nonalcoholic steatohepatitis: The central role of nontriglyceride fatty acid metabolites. *Hepatology*, *52*(2), 774–788. http://doi.org/10.1002/hep.23719

Niimi, S., Horikawa, M., Seki, T., Ariga, T., Kobayashi, T., & Hayakawa, T. (2002). Effect of activins AB and B on DNA synthesis stimulated by epidermal growth factor in primary cultured rat hepatocytes. *Biological & Pharmaceutical Bulletin*, *25*(4), 437–40. http://doi.org/10.1248/bpb.25.437

Nishikawa, H., & Osaki, Y. (2015). Liver Cirrhosis: Evaluation, Nutritional Status, and Prognosis. *Mediators of Inflammation*, *2015*. http://doi.org/10.1155/2015/872152

Nissinen, T. A., Degerman, J., Räsänen, M., Poikonen, A. R., Koskinen, S., Mervaala, E., … Hulmi, J. J. (2016). Systemic blockade of ACVR2B ligands prevents chemotherapy-induced muscle wasting by restoring muscle protein synthesis without affecting oxidative capacity or atrogenes. *Scientific Reports*, *6*(August), 32695. http://doi.org/10.1038/srep32695

Oertel, M., & Shafritz, D. A. (2008). Stem cells, cell transplantation and liver repopulation. *Biochimica et Biophysica Acta (BBA) - Molecular Basis of Disease*, *1782*(2), 61–74. http://doi.org/10.1016/j.bbadis.2007.12.004

Ogawa, Y., Imajo, K., Yoneda, M., Kessoku, T., Tomeno, W., Shinohara, Y., … Nakajima, A. (2013). Soluble CD14 Levels Reflect Liver Inflammation in Patients with Nonalcoholic Steatohepatitis. *PLoS ONE*, *8*(6). http://doi.org/10.1371/journal.pone.0065211

Ooe, H., Chen, Q., Kon, J., Sasaki, K., Miyoshi, H., Ichinohe, N., … Mitaka, T. (2012). Proliferation of rat small hepatocytes requires follistatin expression. *Journal of Cellular Physiology*, *227*(6), 2363–2370. http://doi.org/10.1002/jcp.22971

Palin, N. K., Savikko, J., Pasternack, A., Rintala, J. M., Kalra, B., Mistry, S., … Ritvos, O. (2016). Activin inhibition limits early innate immune response in rat kidney allografts - a pilot study. *Transplant International : Official Journal of the European Society for Organ Transplantation*. http://doi.org/10.1111/tri.12876

Patella, S., Phillips, D. J., Tchongue, J., de Kretser, D. M., & Sievert, W. (2006). Follistatin attenuates early liver fibrosis: effects on hepatic stellate cell activation and hepatocyte apoptosis. *American Journal of Physiology. Gastrointestinal and Liver Physiology*, *290*(1), G137-44. http://doi.org/10.1152/ajpgi.00080.2005

Plank, L. D., & Russell, K. (2015). Nutrition in liver transplantation: too little or too much? *Current Opinion in Clinical Nutrition & Metabolic Care*, *18*(5). JOUR. Retrieved from http://journals.lww.com/co-clinicalnutrition/Fulltext/2015/09000/Nutrition_in_liver_transplantation___too_little_or.14.aspx

Polyzos, S. A., Kountouras, J., Anastasilakis, A. D., Triantafyllou, G. A., & Mantzoros, C. S. (2016). Activin A and follistatin in patients with nonalcoholic fatty liver disease. *Metabolism*, *65*(10), 1550–1558. http://doi.org/10.1016/j.metabol.2016.07.009

Poniatowski, Ł. A., Wojdasiewicz, P., Gasik, R., & Szukiewicz, D. (2015). Transforming growth factor Beta family: insight into the role of growth factors in regulation of fracture healing biology and potential clinical applications. *Mediators of Inflammation*, *2015*, 137823. http://doi.org/10.1155/2015/137823

Rinella, M. (2015). Nonalcoholic Fatty Liver Disease. *N Engl J Med*, *346*(16), 1221–1231. http://doi.org/10.1007/978-1-4939-0548-5_10

Rodriguez, J., Vernus, B., Chelh, I., Cassar-Malek, I., Gabillard, J. C., Hadj Sassi, A., … Bonnieu, A. (2014). Myostatin and the skeletal muscle atrophy and hypertrophy signaling pathways. *Cellular and Molecular Life Sciences*. http://doi.org/10.1007/s00018-014-1689-x

Safadi, R., & Friedman, S. L. (2002). Hepatic fibrosis--role of hepatic stellate cell activation. *MedGenMed : Medscape General Medicine*, *4*(3), 27.

Sakai, K., Jawaid, S., Sasaki, T., Bou-Gharios, G., & Sakai, T. (2014). Transforming Growth Factor-β-Independent Role of Connective Tissue Growth Factor in the Development of Liver Fibrosis. *The American Journal of Pathology*, *184*(10), 2611–7. http://doi.org/10.1016/j.ajpath.2014.06.009

Sakhuja, P. (2014). Pathology of alcoholic liver disease, can it be differentiated from nonalcoholic steatohepatitis? *World Journal of Gastroenterology*, *20*(44), 16474–16479. http://doi.org/10.3748/wjg.v20.i44.16474

Sako, D., Grinberg, A. V., Liu, J., Davies, M. V., Castonguay, R., Maniatis, S., … Kumar, R. (2010). Characterization of the ligand binding functionality of the extracellular domain of activin receptor type IIB. *Journal of Biological Chemistry*, *285*(27), 21037–21048. http://doi.org/10.1074/jbc.M110.114959

Sartori, R., Milan, G., Patron, M., Mammucari, C., Blaauw, B., Abraham, R., & Sandri, M. (2009). Smad2 and 3 transcription factors control muscle mass in adulthood. *Am J Physiol Cell Physiol*, *296*(6), C1248-57. http://doi.org/10.1152/ajpcell.00104.2009

Schaap, F. G., Kremer, A. E., Lamers, W. H., Jansen, P. L. M., & Gaemers, I. C. (2013). Fibroblast growth factor 21 is induced by endoplasmic reticulum stress. *Biochimie*, *95*(4), 692–699. http://doi.org/10.1016/j.biochi.2012.10.019

Schwall, R. H., Robbins, K., Jardieu, P., Chang, L., Lai, C., & Terrell, T. G. (1993). Activin induces cell death in hepatocytes in vivo and in vitro. *Hepatology (Baltimore, Md.)*, *18*(2), 347–56. http://doi.org/S0270913993001880 [pii]

Seki, E., & Brenner, D. A. (2015). Recent advancement of molecular mechanisms of liver fibrosis. *Journal of Hepato-Biliary-Pancreatic Sciences*, 512–518. http://doi.org/10.1002/jhbp.245

Seki, E., & Schwabe, R. F. (2015). Hepatic inflammation and fibrosis: Functional links and key pathways. *Hepatology*, *61*(3), 1066–1079. http://doi.org/10.1002/hep.27332

Sinclair, M., Grossmann, M., Hoermann, R., Angus, P. W., & Gow, P. J. (2016). Testosterone therapy increases muscle mass in men with cirrhosis and low testosterone: A randomised controlled trial. *J Hepatol*. http://doi.org/10.1016/j.jhep.2016.06.007

Smith, R. C., Cramer, M. S., Mitchell, P. J., Capen, A., Huber, L., Wang, R., … Heuer, J. G. (2015). Myostatin Neutralization Results in Preservation of Muscle Mass and Strength in Preclinical Models of Tumor-Induced Muscle Wasting. *Molecular Cancer Therapeutics*, *14*(7), 1661–1670. http://doi.org/10.1158/1535-7163.MCT-14-0681

Szláma, G., Trexler, M., & Patthy, L. (2013). Latent myostatin has significant activity and this activity is controlled more efficiently by WFIKKN1 than by WFIKKN2. *FEBS Journal*, *280*(16), 3822–3839. http://doi.org/10.1111/febs.12377

Tag, C. G., Sauer-Lehnen, S., Weiskirchen, S., Borkham-Kamphorst, E., Tolba, R. H., Tacke, F., & Weiskirchen, R. (2015). Bile Duct Ligation in Mice: Induction of Inflammatory Liver Injury and Fibrosis by Obstructive Cholestasis. *Journal of Visualized Experiments*, (February), 1–11. http://doi.org/10.3791/52438

Terpos, E., Kastritis, E., Christoulas, D., Gkotzamanidou, M., Eleutherakis-Papaiakovou, E., Kanellias, N., … Dimopoulos, M. A. (2012). Circulating activin-A is elevated in patients with advanced multiple myeloma and correlates with extensive bone involvement and inferior survival; no alterations post-lenalidomide and dexamethasone therapy. *Annals of Oncology*, *23*(10), 2681–2686. http://doi.org/10.1093/annonc/mds068

Tilg, H., & Moschen, A. R. (2010). Evolution of inflammation in nonalcoholic fatty liver disease: The multiple parallel hits hypothesis. *Hepatology*, *52*(5), 1836–1846. http://doi.org/10.1002/hep.24001

Timchenko, N. A. (2009). Aging and liver regeneration. *Trends in Endocrinology and Metabolism*. http://doi.org/10.1016/j.tem.2009.01.005

Trendelenburg, A. U., Meyer, A., Rohner, D., Boyle, J., Hatakeyama, S., & Glass, D. J. (2009). Myostatin reduces Akt/TORC1/p70S6K signaling, inhibiting myoblast differentiation and myotube size. *American Journal of Physiology. Cell Physiology*, *296*(April 2009), C1258–C1270. http://doi.org/10.1152/ajpcell.00105.2009

Tsuchida, K. (2004). Activins, myostatin and related TGF-beta family members as novel therapeutic targets for endocrine, metabolic and immune disorders. *Current Drug Targets. Immune, Endocrine and Metabolic Disorders*, *4*(2), 157–66. http://doi.org/10.2174/1568008043339901

Tsuchida, K. (2008). Targeting myostatin for therapies against muscle-wasting disorders. *Current Opinion in Drug Discovery & Development*, *11*(4), 487–94. Retrieved from http://www.ncbi.nlm.nih.gov/pubmed/18600566

Wada, W., Maeshima, A., Zhang, Y.-Q., Hasegawa, Y., Kuwano, H., & Kojima, I. (2004). Assessment of the function of the betaC-subunit of activin in cultured hepatocytes. *American Journal of Physiology. Endocrinology and Metabolism*, *287*(2), E247-54. http://doi.org/10.1152/ajpendo.00390.2003

Wagner, K. R., McPherron, A. C., Winik, N., & Lee, S. J. (2002). Loss of myostatin attenuates severity of muscular dystrophy in mdx mice. *Annals of Neurology*, *52*(6), 832–836. http://doi.org/10.1002/ana.10385

Wagner, K. R., RA, P., Bird, T., Dolan, C., Stephens, K., & Adams, M. (1993). Myostatin-Related Muscle Hypertrophy. *GeneReviews*.

Wang, D. H., Wang, Y. N., Ge, J. Y., Liu, H. Y., Zhang, H. J., Qi, Y., … Cui, X. L. (2013). Role of activin A in carbon tetrachloride-induced acute liver injury. *World Journal of Gastroenterology*, *19*(24), 3802–3809. http://doi.org/10.3748/wjg.v19.i24.3802

Weber, L. W. D., Boll, M., & Stampfl, A. (2003). Hepatotoxicity and mechanism of action of haloalkanes: carbon tetrachloride as a toxicological model. *Critical Reviews in Toxicology*, *33*(2), 105–136. http://doi.org/10.1080/713611034

Xiong, J., Shang, W., Wu, L., Chen, R., Liu, W., Ning, R., … Yang, J. (2014). Glucose dominates the regulation of carboxylesterases induced by lipopolysaccharide or interleukin-6 in primary mouse hepatocytes. *Life Sciences*, *112*(1–2), 41–48. http://doi.org/10.1016/j.lfs.2014.07.019

Xu, F., Liu, C., Zhou, D., & Zhang, L. (2016). TGF-β/SMAD Pathway and Its Regulation in Hepatic Fibrosis. *The Journal of Histochemistry and Cytochemistry : Official Journal of the Histochemistry Society*, *64*(3), 157–67. http://doi.org/10.1369/0022155415627681

Yaden, B. C., Wang, Y. X., Wilson, J. M., Culver, A. E., Milner, A., Datta-Mannan, A., … Krishnan, V. (2014). Inhibition of activin a ameliorates skeletal muscle injury and rescues contractile properties by inducing efficient remodeling in female mice. *American Journal of Pathology*, *184*(4), 1152–1166. http://doi.org/10.1016/j.ajpath.2013.12.029

Yin, C., & Evason, K. (2013). Hepatic stellate cells in liver development, regeneration, and cancer. *The Journal of Cinical Investigation*, *123*(5), 1902–1910. http://doi.org/10.1172/JCI66369.1902

Yndestad, A., Haukeland, J. W., Dahl, T. B., Bjøro, K., Gladhaug, I. P., Berge, C., … Aukrust, P. (2009). A complex role of activin A in non-alcoholic fatty liver disease. *The American Journal of Gastroenterology*, *104*(December 2008), 2196–205. http://doi.org/10.1038/ajg.2009.318

Zhang, Y., Feng, X.-H., We, R., & Derynck, R. (1996). Receptor-associated Mad homologues synergize as effectors of the TGF-beta response. *Nature*. http://doi.org/10.1038/383168a0